

Research Article

The Pleistocene ice-sheet dynamics in north-central Poland based on magnetic fabrics of tills and landform analysis

Artur Teodorski 

Doctoral School of Exact and Natural Sciences, University of Warsaw, 02-097 Warsaw, Poland

Abstract

This research was carried out in north-central Poland, which was occupied by the ice sheet of the Saalian (Marine Isotope Stage [MIS] 6) and Upper Stadial of the Weichselian (MIS 2) glaciation. The application of the anisotropy of magnetic susceptibility (AMS) method supported by a digital elevation model (DEM) analysis of the orientation of glacial landforms allowed for the reconstruction of ice-sheet extent and ice movement directions of these two Pleistocene glaciations. The research used an innovative method of collecting AMS till samples from the glacial plateau areas. Based on the research, it was found that during the general recession of the ice sheet of the Saalian glaciation, a previously undescribed glacial transgression occurred, characterized by a different direction of ice-sheet movement. On the basis of detailed geomorphological studies of the area of terminal moraines, previously described in fragments, the maximum extent of the ice sheet during the Weichselian glaciation was clarified. The recession of the ice sheet of the Weichselian glaciation from the area of north-central Poland took place in four regressive or transgressive–regressive stages with variable directions of ice-sheet movement. The results obtained indicate the great potential of the AMS method in paleoenvironmental studies of glaciated areas.

Keywords: Pleistocene, Saalian glaciation, Weichselian glaciation, North-central Poland, Magnetic fabric, Geomorphology

(Received 13 May 2023; accepted 8 January 2024)

Introduction

Geologic studies concerning ice-sheet extent and directions of ice movement constitute an important branch of Quaternary research (e.g., Stokes et al., 2015). They allow us to understand the mechanism of advance and retreat of ice sheets during individual glaciations. The digital elevation model (DEM) has become a particularly useful tool for this type of research (Clark, 1997; Jorgensen and Piotrowski, 2003; Raunholm et al., 2003; Ewertowski and Rzeszewski, 2006; King et al., 2016; Rychel and Morawski, 2017; Teodorski, 2023). However, there are cases (e.g., connected with postglacial processes like erosion) in which the glacial relief is not well developed enough to make conclusions about the directions of the ice-sheet movement. A second useful method for determining the local direction of ice-sheet movement is the analysis of pebble fabric in tills. The use of this method, however, has a major limitation, because it depends on the number of till exposures available. The textural features of the tills, indicated by the arrangement of the pebbles, are also present in the microscale. An effective tool for measuring the average orientation of fine grains is the anisotropy of magnetic susceptibility (AMS) method, which has been used to determine not only the directions of movement, but also the mechanism of ice-sheet movement, and to reconstruct processes of subglacial till formation. This method of studying tills has been refined across more

than six decades of use (e.g., Fuller, 1962; Stupavsky and Gravenor, 1975; Stewart et al., 1988; Hooyer et al., 2008; Thomason and Iverson, 2009; Gentoso et al., 2012; Fleming et al., 2013; Tylmann et al., 2013; Ankerstjerne et al., 2015; Król and Wachecka-Kotkowska, 2015; Hopkins et al., 2016; McCracken et al., 2016; Narloch et al., 2021; Teodorski et al., 2021).

The aim of this research was to reconstruct the directions of ice advance and pattern of its retreat during the Saalian (Marine Isotope Stage [MIS] 6) and Upper Stadial of the Weichselian (MIS 2) glaciation in the study area in north-central Poland. The AMS method was used for the study, supported by the DEM analysis. An original method of collecting AMS till samples from the areas of glacial plateaus was used. This quick method of sampling, combined with the further development of the AMS measurement technique, makes it possible to determine the directions of ice-sheet movement in any area with near-surface layers of glacial tills and where there are no exposures of these tills. The results of the research provided new information on the glacial history of this part of Poland, in particular on the extent, direction of movement, advance, and retreat of ice sheets during the Saalian and Weichselian glaciations.

Geomorphological and geological settings

The research area is located in north-central Poland. Its eastern part belongs to the Płoński Plateau (Fig. 1B), which is part of the North Mazovian Lowland (Solon et al., 2018). Elevation ranges here from 114 m above sea level (asl) in the northern part, adjacent to the Raciąż Plain, to 164 m asl in the central

Email: a.teodorski@student.uw.edu.pl

Cite this article: Teodorski A (2024). The Pleistocene ice-sheet dynamics in north-central Poland based on magnetic fabrics of tills and landform analysis. *Quaternary Research* 119, 99–117. <https://doi.org/10.1017/qua.2024.2>

© The Author(s), 2024. Published by Cambridge University Press on behalf of Quaternary Research Center



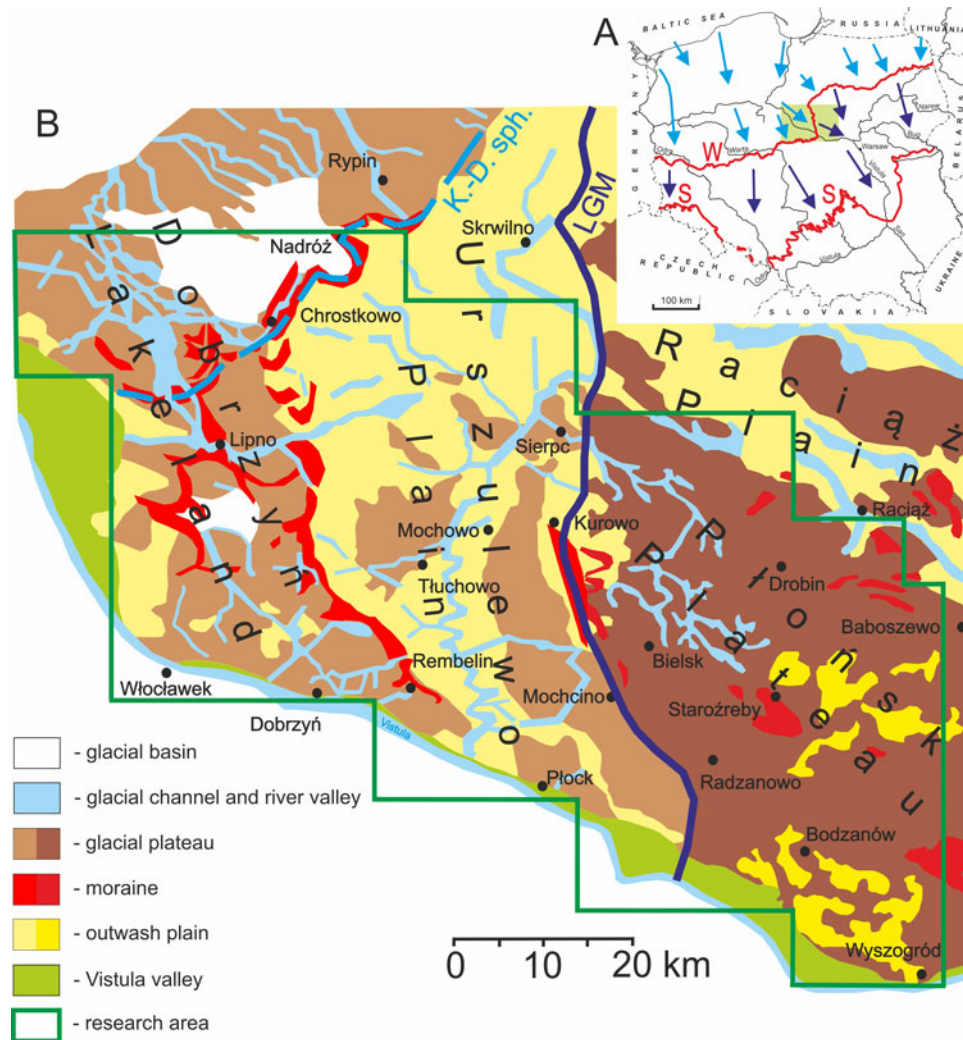


Figure 1. (A) Location of the study area (green rectangle) against the extent of the ice sheet during the Saalian (S) and Weichselian (W) glaciations and their directions of ice-sheet movement (after Marks et al., 2016, 2018, 2022); (B) geomorphological map of the study area. LGM, the maximum extent of the Weichselian glaciation ice sheet (according to Dzierżek, 2009; Marks et al., 2022); K.-D. sph., Kujawy-Dobrzyń subphase (after Niewiarowski et al., 1995).

part, and it drops again toward the south to 84 m asl. Most of the study area is a glacial plateau. Small areas are occupied by fluvioglacial deposits, mainly in the western (south of Sierpc), central (east of Staroźreby), and southern (northwest of Wyszogród) parts of the area. Several sequences of terminal moraines have also been identified in this region.

The western part of the study area belongs to the Dobrzyń Lakeland (Fig. 1B), which is part of the Chełmno-Dobrzyń Lakeland (Solon et al., 2018). Elevation in this region ranges from 57 to 146 m asl. It is also a glacial plateau, except for small fragments of land in the western and southern parts that are occupied by fluvioglacial deposits. The characteristic elements of the glacial relief of the Dobrzyń Lakeland are numerous arcs of terminal moraines that have been described by many other researchers (e.g., Nechay, 1927; Lamparski, 1991; Dzierżek, 2009; Teodorski, 2023). They mark the location of the paleo-ice sheet front during the last deglaciation. Another characteristic element of the glacial relief is a conspicuous network of glacial meltwater channels.

Both areas of glacial plateau are separated from each other by the Urszulewo Plain, also belonging to the Chełmno-Dobrzyń Lakeland (Solon et al., 2018; Fig. 1B). Its flat surface slopes

from north to south, from 135 to 81 m asl. It is an outwash plain built of fluvioglacial deposits.

The area of the Płońsk Plateau was last covered by an ice sheet during the Warta stadial of the Saalian glaciation (MIS 6) (Marks et al., 2016; Fig. 1A). Several sequences of terminal moraines occur here, reflecting successive stages of ice-sheet recession. Moraine hills are known from the area north of Wyszogród, near Staroźreby or Raciąż (Baraniecka, 1996; Kacprzak and Lisicki, 2005; Kucharska and Wasiluk, 2005; Frankiewicz, 2009; Różański and Włodek, 2009; Fig. 1B). In the west, they occur between the villages of Kurowo, Mochcino, and Bielsk (Lamparski, 1978; Dzierżek, 2009).

The western part of the study area (Dobrzyń Lakeland and Urszulewo Plain) was last covered by the Płock Lobe of the Weichselian ice sheet (Rühle, 1957; Skompski, 1969; Marks, 1988, 2022; Mojski, 2005; Dzierżek, 2009; Roman, 2010; Marks et al., 2016; Fig. 1A). The last glacial maximum (LGM) in this part of Poland falls in the Poznań phase, dated to 20–19 ka (Marks et al., 2016, 2022). On the other hand, the latest ^{10}Be exposure dating shows that the local LGM in western and central Poland is ca. 25–21 ka, and ice-sheet retreat from the extent of Poznań phase began at 17.3 ± 0.5 ka (Tylmann et al., 2019). The Poznań phase

is correlated with the Frankfurt phase in Germany and the Grūda phase in Lithuania (Marks, 2012). The extent of the ice sheet during the local LGM is not definitive at this time, due to the few hills of terminal moraines that could confirm its extent. According to Kotarbiński (1998), in the area of Sierpc and to the north of it (outside the study area), there are single moraine hills that were deposited during the Weichselian glaciation. Dzierżek (2009) indicates the existence of terminal moraines from the local LGM period on the Mochcino-Kurowo line (Fig. 1B), which was also pointed out by Lamparski (1978). Roman (2019) reconstructs the extent of the last ice sheet based on moraines in Mikołajewo (east of Płock) and moraine hills northwest of Mochcino, as well as the distribution of outwash plains. She also indicates the presence of overridden moraines in the hinterland of the local LGM ice limit, which were originally formed before the maximum extent of the ice sheet during the Weichselian glaciation. Róžański and Włodek (2009) also draw attention to the existence of moraines in Mikołajewo. In the Urszulewo Plain, due to meltwater erosion and accumulation of fluvio-glacial sediments, it is difficult to trace the successive recessional limits of the ice sheet. Roman (2019) recognized the presence of overridden moraines from the pre-maximum period in the area to the northwest of Płock. Numerous sequences of terminal moraines in the Dobrzyń Lakeland reflect the extent of individual glacial lobes that formed during successive phases of the last deglaciation (Lamparski, 1991, 2001; Dzierżek, 2009; Teodorski, 2023). Moraines in the northern part of the region indicate the extent of the transgressive–regressive Kujawy–Dobrzyń subphase (Fig. 1B), which has been dated at 17.7 ka BP (Kozarski, 1995; Wysota et al., 2002).

The tills forming the surface parts of the study area were examined. The Płoński Plateau is built of sediments belonging to the Saalian glaciation. The thickness of these sediments exceeds 100–110 m in the central part of the plateau (Kacprzak and Lisicki, 2011; Róžański and Włodek, 2012). These are mainly glacial tills, ice-dammed sediments, and fluvio-glacial sands and gravels (e.g., layers 3–14 of profile I–J in Fig. 2). Glacial tills belonging to the Warta Stadial of the Saalian glaciation are exposed on the terrain surface (MIS 6; Baraniecka, 1996; Frankiewicz, 2009; Kacprzak and Lisicki, 2011; Róžański and Włodek, 2012; layer 7 of profile I–J, as well as layer 12 of other profiles). They usually reach a thickness of several meters, up to a maximum of 30–40 m in the central part of the plateau.

The Dobrzyń Lakeland and Urszulewo Plain areas are built of sediments accumulated during the Weichselian glaciation. In the Lakeland area, these deposits reach from several meters (in the northern and western parts; Lamparski, 1985; Dzierżek, 2006) to more than 70 m, north of Mochowo (Dzierżek and Szymanek, 2009) and mainly consist of glacial tills, ice-dammed sediments, and fluvio-glacial sands and gravels. On the profiles in Figure 2, the sediments belonging to the Weichselian glaciation are represented by layers 18–33. Glacial tills deposited during the Upper Stadial of the Weichselian glaciation are exposed on the surface of the glacial plateau (MIS 2; Lamparski, 1978, 1980, 1985; Dzierżek, 2006; Róžański and Włodek, 2012). The thickness of these tills generally reaches 15 m.

Methods

Analysis of the DEM

The DEM used for the study was generated on the point cloud basis with a horizontal resolution of 1 m, obtained on the basis

of light detection and ranging (LIDAR) scanning of the terrain surface. Elevation data come from the resources of the Head Office of Geodesy and Cartography in Warsaw. QGIS 3 was used to generate the model. To determine the origin of the glacial forms, individual sheets of the Detailed Geological Map of Poland at the scale of 1:50,000 were analyzed (Mojski, 1958; Skompski and Słowański, 1962; Skompski, 1968; Łyczewska, 1973; Lamparski, 1978, 1980, 1985; Baraniecka, 1996; Kotarbiński, 1998; Kacprzak and Lisicki, 2005; Kucharska and Wasiluk, 2005; Dzierżek, 2006; Wysota, 2006; Dzierżek and Szymanek, 2009; Frankiewicz, 2009; Róžański and Włodek, 2009; Wysota and Sokołowski, 2009). The analysis of the DEM was carried out for the purpose of determining the orientations of glacial landforms in the study area.

Grain-size analysis

Wet-sieving tests (Mycielska-Dowgiałło and Rutkowski, 1995) were carried out on 33 samples of glacial tills at 1.5–2.0 m depths. A sample weighing 200 g, taken from drilling samples, was sieved under running water on a set of 11 sieves with the following diameters: 10, 4, 2, 1, 0.8, 0.355, 0.2, 0.125, 0.1, and 0.063 mm.

Petrographic analysis of the gravel fraction (5–10 mm)

Thirty-three samples of glacial till at 1.5–2.0 m depths and weighing 2 kg, taken from drilling samples, were used for the study, from which a gravel fraction with a diameter of 5–10 mm was separated. From each sample, at least 100 grains were analyzed (according to the procedure of Lisicki [2003]), which were classified as Scandinavian rocks (crystalline rocks and northern quartz, limestones, dolomites, sandstones and quartzites, and northern shales) or local rocks (limestones and marls, sandstones, mudstones, and claystones, as well as other local rocks like flints and lydites). Due to the vast predominance of crystalline rocks and/or northern limestones and small percentage changes in other types of rocks, only two main types of rocks are described in the results.

Collection of AMS samples

AMS samples were taken from near-surface layers of glacial tills forming areas of postglacial plateau. The sampling procedure was as follows: (1) drilling a maximum depth of 2 m using a handheld Eijkelkamp probe (two to three drilling holes per site), (2) AMS sampling using a 15-cm-long and 2.54-cm-diameter brass sampler (Fig. 3A) from a depth of 1.5–2.0 m, driven vertically into the bottom of the hole. This sampling depth was adopted due to the possible disturbance of sediments in the upper layers as a result of frost processes or biogenic or human activity. Unfortunately, the handheld Eijkelkamp probe does not allow tracing any undisturbed sedimentary structures of tills located above 2 m depth. The z-axis line and the direction of the north were marked on the brass sampler. Before the probe was removed from the hole, the azimuth and the angle of inclination of the probe axis were measured. Then, the till cores were pushed out from the sampler. The obtained till cores were cut to the standard size for AMS cylindrical specimens (2 cm long and 2.54 cm wide; Fig. 3B and C). They were oriented relative to a 3D coordinate system with z- and x-axes marked on their surfaces. On average, two to five AMS samples were obtained from one core, and four

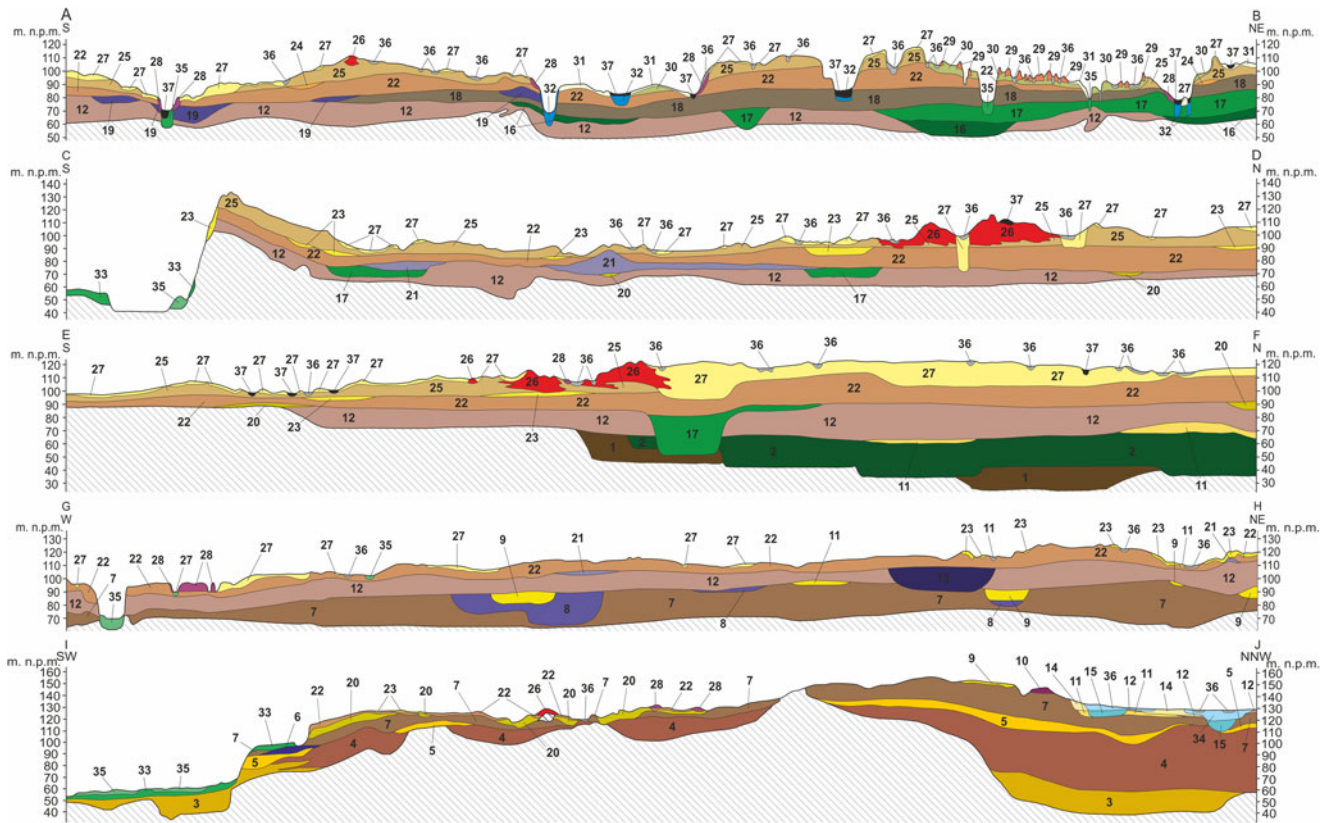


Figure 2. Representative geologic cross sections in the study area (based on Lamparski, 1980, 1985; Dzierżek, 2006; Rózański and Włodek, 2012; Frankiewicz, 2013). Locations of the cross sections on the Fig. 4. **Elsterian Glaciation (MIS 12):** 1-glacial tills; **Holsteinian Interglacial (MIS 11):** 2-fluvial sands with gravels, sands, silts and clays; **Saalian Glaciation, Main Stadial (MIS 6):** 3-fluvioglacial sands, 4-glacial tills; **Saalian Glaciation, Warta Stadial (MIS 6):** 5-fluvioglacial sands and gravels, 6-ice-dammed silts and clays, 7-glacial tills, 8-ice-dammed sands and silts, 9-fluvioglacial sands and gravels, 10-silts, sands and clays of kames, 11-fluvioglacial sands and gravels, 12-glacial tills, 13-ice-dammed sands and silts, 14-fluvioglacial sands with gravels; **Eemian Interglacial (MIS 5e):** 15-limnic silts, gyttjas and peats, 16-fluvial sands and gravels, 17-fluvial sands and silts; **Weichselian Glaciation, Middle Stadial (MIS 4):** 18-glacial tills, 19-ice-dammed clays; **Weichselian Glaciation, Upper Stadial (MIS 2):** 20-fluvioglacial sands, 21-ice-dammed silts and sands; 22-glacial tills, 23-fluvioglacial sands, 24-limnic and fluvial silts, sandy clays and sands; 25-glacial tills; 26-sands and gravels of moraine hills; 27-fluvioglacial sands and gravels; 28-sands and silts of kames and kame terraces; 29-tills, gravels and silts of glacial curvilinearations; 30-flow tills; 31-fluvioglacial sands; 32-limnic sands; 33-fluvial sands, gravels and silts; **Weichselian Glaciation/Holocene (MIS 2/MIS 1):** 34-limnic and fluvial sands and silts; **Holocene MIS 1:** 35-fluvial sands; 36-muds; 37-peats.

cores in two to three drilling holes were obtained from each site. In this particular site, each hole is about 1–2 m away from the next one. The total number of samples collected was 458 pieces.

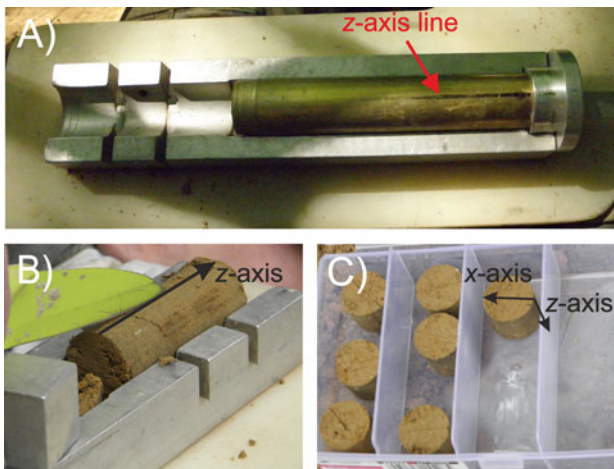


Figure 3. Examples of anisotropy of magnetic susceptibility (AMS) sample collection: (A) brass sampler with z-axis line and north direction (black line); (B) till core with z-axis line on the top; (C) individual AMS samples with z- and x-axes lines.

Anisotropy of magnetic susceptibility (AMS)

The AMS of the samples was measured using the MFK1-FA Kappabridge (Agico) with a 3D rotator and Safyr 7 software. Magnetic susceptibility measurements were carried out in a field with an intensity of 200 A/m and a frequency of 976 kHz. AMS measurements were carried out at the European Center for Geological Education in Chęciny (Poland).

To visualize the data, stereographic projections to the lower hemisphere in the geographic coordinate system generated with Anisoft 5 were used. The projections show the orientation of the principal axes of magnetic susceptibility—maximum (k_{\max}), intermediate (k_{int}), and minimum (k_{\min}). The mean orientations of the individual susceptibility axes with their confidence ellipsoids were calculated on the basis of Jelínek (1978). To describe the susceptibility and its anisotropy for individual samples, the following parameters were calculated: mean magnetic susceptibility [$K_m = (k_{\max} + k_{\text{int}} + k_{\min})/3$]; magnetic lineation [$L = k_{\max}/k_{\text{int}}$]; magnetic foliation [$F = k_{\text{int}}/k_{\min}$]; corrected degree of anisotropy [$P_j = (k_{\max}/k_{\min})^a$], where $a = \sqrt{(1 + T^2)/3}$; and the shape parameter [$T = (2\eta_2 - \eta_1 - \eta_3)/(\eta_1 - \eta_3)$], where $\eta_1 = \ln k_{\max}$, $\eta_2 = \ln k_{\text{int}}$, $\eta_3 = \ln k_{\min}$ (Hroudá, 1982). Before the AMS projection was interpreted, the available results were filtered. The values K_m and P_j were selected for filtration. The filtration was based on the median

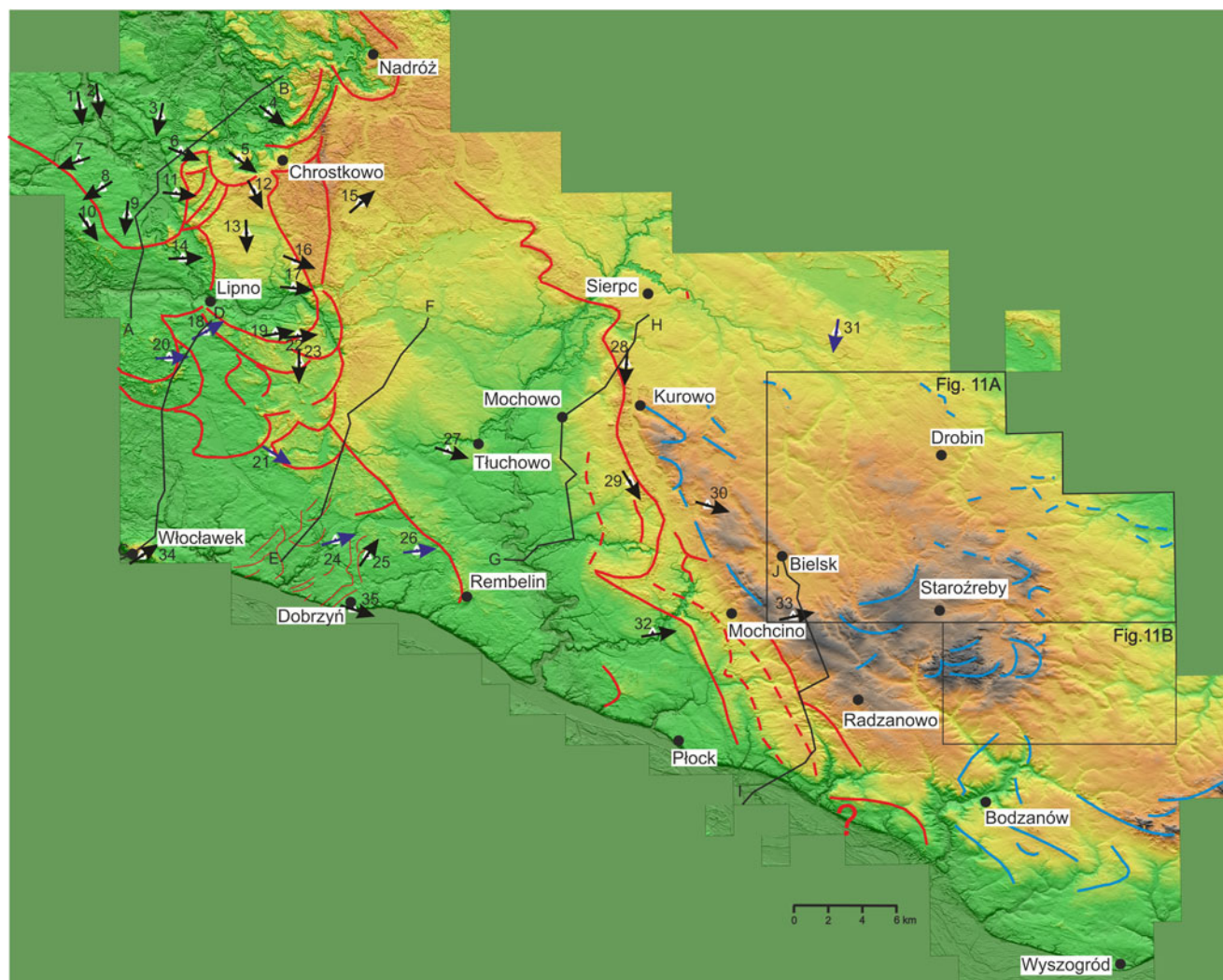


Figure 4. Location of the anisotropy of magnetic susceptibility (AMS) sites (triangles) along with the interpreted direction of ice-sheet movement (arrows: black are $S_1 \geq 0.6$, well oriented axes; blue are $S_1 < 0.6$, weakly oriented axes) against the background of the digital elevation model (DEM) and the location of sequences of terminal moraine forms (continuous lines, sequences of terminal moraines; dashed lines, sequences of overridden moraines; blue lines, sequences of moraines from the Saalian glaciation; red lines, sequences of moraines from the Weichselian glaciation); see Table 1 for names and numbers of sites.

and 25% and 75% quartiles. Samples above the level described by the formula $Q3 + 1.5 \times IQR$, where $Q3$ is the 75% quartile, and IQR is the interquartile range between the 25% and 75% quartiles, were removed due to anomalously high values of the parameters (Hodge and Austin, 2004; Stachowska et al., 2020; Teodorski et al., 2021). The IQR outliers method is not dependent on abnormally high boundary values, unlike the standard deviation method. This method depends only on the 25th and 75th percentiles, which means that it measures the spread of the middle 50% of the results of a given set. According to this author, this method allows for better filtration of abnormally high AMS parameter values. A sample with such high AMS parameter values can significantly affect the magnetic fabric of a given site. Extremely high parameter values may be associated, for example, with the occurrence of rock fragments with high AMS anisotropy. As a result of filtration, 68 samples were removed, which is about 15% of all measured samples. The obtained AMS results were subjected to statistical analysis that consisted of determining the degree of spatial orientation of the maximum and minimum magnetic susceptibility axes. For each set of orientations of the susceptibility axes,

the eigenvector v_1 was determined (Woodcock, 1977), which estimates the mean direction of the axes and the eigenvalue of this vector, λ_1 . To determine the grouping of the axes around the mean vector, the normalized eigenvalues S_1 were calculated based on the formula $S_1 = \lambda_1/N$, where $S_1 < 1$ (Woodcock, 1977). In the present paper, it was assumed that certain statistically mean directions of the susceptibility axis are obtained when $S_1 \geq 0.6$. When S_1 is below 0.6, the axes are poorly oriented. However, if the determined direction is confirmed by the orientation of glacial landforms, it is used in the interpretation with caution. In addition, the value of the S_1 eigenvalue for the orientation of the maximum susceptibility axis may indicate the magnitude of the action of shear forces during the deposition of glacial tills (Hooyer et al., 2008).

Rock magnetism analysis

The selected AMS samples were used for all rock magnetism analyses. For the initial determination of the type of magnetic minerals, S-ratio measurements were carried out. In the first step, a

Table 1. Anisotropy of magnetic susceptibility (AMS) measurement results.^a

Sample site ^b	na/nf	K_m ($\times 10^{-4}$ SI)	L (-)	F (-)	P_j (-)	T (-)	D/I (°)			S_1 (-)		IDSM (°)	S ratio (-)
							k_{max}	k_{int}	k_{min}	k_{max}	k_{min}		
1. Mazowsze	8/8	2.26	1.015	1.009	1.024	-0.248	172/11	82/2	344/79	0.634	0.621	172	0.23
2. Kijaszkowo	15/13	2.73	1.011	1.003	1.014	-0.534	173/8	270/43	75/46	0.634	0.593	173	0.12
3. Klonowo	13/10	1.90	1.007	1.003	1.010	-0.439	12/14	142/70	278/15	0.645	0.532	192	0.18
4. Nowa Wieś	12/10	2.41	1.008	1.009	1.017	0.045	33/7	293/54	128/35	0.542	0.631	128	0.22
5. Wildno	12/11	1.78	1.007	1.011	1.018	0.243	30/20	251/64	126/15	0.603	0.629	126	0.08
6. Moszczonne	14/13	2.65	1.008	1.010	1.018	0.104	197/3	288/14	96/76	0.676	0.738	112	0.04
7. Steklin	11/8	1.73	1.000	1.012	1.015	0.929	344/8	80/35	243/54	0.533	0.834	252	0.18
8. Wawrzonkowo	11/8	1.86	1.011	1.002	1.014	-0.726	238/23	131/35	355/46	0.654	0.522	238	0.22
9. Sumin	8/8	2.13	1.010	1.006	1.016	-0.257	186/6	278/11	69/77	0.733	0.603	186	0.23
10. Makowiska	12/9	1.72	1.008	1.007	1.015	-0.039	146/4	239/38	52/52	0.603	0.559	146	0.20
11. Kikoł	9/7	1.99	1.004	1.005	1.009	0.191	275/19	6/3	104/71	0.442	0.658	96	0.16
12. Janowo	10/7	0.97	1.002	1.001	1.003	-0.412	153/6	27/80	244/8	0.624	0.574	153	0.05
13. Chlebowo	14/14	2.56	1.004	1.014	1.019	0.581	267/4	176/19	10/71	0.513	0.736	178	0.19
14. Złotopole	13/10	2.11	1.005	1.013	1.018	0.422	176/3	86/6	293/83	0.588	0.731	88	0.35
15. Łąkie	10/9	2.34	1.006	1.020	1.028	0.538	142/1	232/9	49/81	0.548	0.758	49	0.14
16. Głogi	15/15	1.91	1.000	1.014	1.016	0.957	303/31	208/8	105/58	0.488	0.627	112	0.12
17. Karnkowo	15/14	2.12	1.011	1.005	1.016	-0.359	276/23	185/2	89/67	0.683	0.578	95	0.05
18. Białowieżyn	10/7	1.08	1.004	1.000	1.005	-0.821	232/27	328/11	77/61	0.556	0.450	61	0.04
19. Głodowo	6/5	1.77	1.008	1.003	1.011	-0.477	81/2	350/23	175/67	0.629	0.624	81	0.09
20. Ignackowo	7/6	1.56	1.003	1.008	1.012	0.463	268/46	359/1	90/44	0.462	0.540	87	0.35
21. Nowa Wieś	11/11	1.88	1.005	1.005	1.010	0.000	215/3	308/41	122/49	0.538	0.587	122	0.19
22. Piątki	14/13	2.33	1.005	1.015	1.020	0.534	270/16	178/6	68/73	0.623	0.785	85	0.02
23. Bałdowo	12/11	1.38	1.002	1.007	1.009	0.644	268/11	172/30	16/58	0.571	0.686	180	-0.06
24. Wierznica	11/9	1.47	1.005	1.007	1.012	0.171	253/4	343/0	74/86	0.481	0.515	73	0.22
25. Mokowo	13/12	2.05	1.003	1.017	1.022	0.720	203/40	107/8	8/49	0.577	0.689	15	0.26
26. Michałkowo	13/9	1.80	1.005	1.005	1.010	-0.047	83/20	343/25	207/57	0.581	0.565	83	0.28
27. Kamień Kotowy	17/14	1.19	1.002	1.003	1.005	0.114	200/1	109/12	295/78	0.535	0.636	108	-0.10
28. Nowe Piastowo	11/9	1.38	1.002	1.006	1.008	0.400	183/23	273/1	5/67	0.510	0.639	184	-0.18
29. Rempin	13/8	2.60	1.005	1.009	1.014	0.296	15/15	281/14	149/69	0.672	0.659	149	0.21
30. Rychacice	15/15	1.35	1.008	1.016	1.024	0.318	197/3	289/36	104/54	0.623	0.656	107	0.07
31. Zawidz Kościelny	15/12	1.02	1.008	1.005	1.013	-0.278	9/24	277/3	180/66	0.549	0.535	189	0.32
32. Stara Biała	13/12	2.35	1.007	1.018	1.026	0.461	254/18	345/2	81/72	0.586	0.733	81	0.16
33. Kuchary-Jeżewo	19/17	1.84	1.011	1.004	1.016	-0.449	78/19	174/18	304/63	0.647	0.513	78	0.42
34. Włocławek	38/33	1.41	1.006	1.021	1.029	0.567	144/1	235/14	49/76	0.583	0.743	56	—
35. Dobrzyń	14/13	1.96	1.004	1.030	1.038	0.757	20/4	111/7	260/82	0.575	0.885	108	—

^aAbbreviations/parameters: na, number of all samples taken; nf, number of samples after filtration; K_m , mean magnetic susceptibility; L , magnetic lineation; F , magnetic foliation; P_j , corrected degree of anisotropy; T , shape parameter; mean orientation of principal susceptibility axes: D , declination; I , inclination; k_{max} , maximum susceptibility axis; k_{int} , intermediate susceptibility axis, k_{min} , minimum susceptibility axis; S_1 , normalized eigenvalue for the susceptibility axis; IDSM, interpreted azimuth of the direction of ice-sheet movement; (SI), magnetic susceptibility unit; (-), unitless.

^bSites where the S_1 eigenvalue for the k_{max} and k_{min} axes are below 0.6 (weakly oriented axes) have been marked in red.

magnetic field of 1 T (IRM_{1T}), was applied along the z-axis, followed by an inverse field of 100 mT (IRM_{-100mT}). The S-ratio was calculated according to the formula $S = -(IRM_{-100mT}/IRM_{1T})$ (Stober and Thomson, 1979; Grabowski et al., 2019).

Thirty-three samples were used for the measurements, one from each location. Measurements of the stepwise acquisition of isothermal remanent magnetization (IRM) were carried out on six samples with different S-ratio values and from different locations.

The magnetic field was applied to the samples along the z-axis in 22 steps of magnetization up to a maximum field value of 3 T. Both analyses allow for determining the relationship of low-coercivity minerals (e.g., magnetite) to high-coercivity minerals (e.g., hematite, goethite) (e.g., Opdyke and Channell, 1996).

The Lowrie test (Lowrie, 1990) was carried out on 10 samples from different locations and with different S-ratio values. Magnetic fields of 1.4 T, 0.4 T, and 0.1 T along the z-, y-, and x-axes were applied to the samples. The samples were then thermally demagnetized in 13 steps, up to 700°C. This test allows for the identification of magnetic minerals on the basis of their Curie temperatures, with the division into minerals with different coercivity.

Anisotropy of anhysteretic remanent magnetization (AARM) was carried out on 25 samples from three locations differing in the *T* parameter value. The ARM was applied in 12 specific directions. In the analysis, an alternating field in the range of 0–100 mT and a steady field of 100 μ T were used. After each cycle of ARM measurements, the samples were demagnetized. An analysis was conducted to determine the types of minerals responsible for AMS (Jackson, 1991).

The magnetic remanent was applied with the LDA5/PAM1 (Agico) pulse magnetizer/demagnetizer for ARM and the MMPM 10 pulse magnetizer (Magnetic Measurements) for IRM. Magnetic remanent was measured using a JR-6A (Agico) spinner magnetometer with Rema 6 software. Measurements of rock magnetism were carried out at the European Center for Geological Education in Chęciny (Poland).

Results

Location and orientation of moraine sequences

Several sequences of terminal moraines have been marked out in the area of the Płoński Plateau. In the SE part of the research area, to the northeast of Wyszogród, there are clearly visible, generally latitudinally oriented moraine hills up to 30 m high (Fig. 4). These moraines are probably extended by the remains of moraine hills near Bodzanów. Another series of terminal moraine hills, although poorly visible on the DEM, is located in the NE part of the study area, southeast of Drobin. It is generally oriented latitudinally, and the maximum height of the hills is 8 m. It shows the extent of the ice-sheet front in the younger recessive episode of the Saalian glaciation. Moraines in the central part of the Płoński Plateau, near Staroźreby, are characterized by an orientation similar to NE-SW. The highest moraine hills reach 28 m in height. Then, farther west, between Mochcino and Kurowo, there are more moraines belonging to the Saalian glaciation. They are oriented along the NNW-SEE line and reach a height of up to 14 m.

In the western part of the Płoński Plateau, several moraine sequences have been preserved, the formation of which can be associated with the local LGM either directly before or after this period (Fig. 4). Between Mochcino, Radzanowo, and Płock, four sequences of forms have been preserved, reflecting the extent and shape of the front of the ice sheet. The first one is located west of Radzanowo, but it is not clearly visible in the terrain. This series includes moraines identified by Różański and Włodek (2009) southwest of Radzanowo. The extension of these forms may be fragmentary remains of moraines preserved to the northwest of Mochcino, measuring up to 11 m high. The next two sequences of forms located south and west of

Mochcino (Fig. 4, dashed line) have a different character. In addition to the NW-SE lines of forms visible in the DEM and up to 10 m high, they are also characterized by the occurrence of a series of elongated hillocks perpendicular to the main lines of forms. The elongated perpendicular hills reach a height of up to 6 m. Similar sequences of forms, although much more badly preserved, have been identified south of Mochowo. The last and longest series of moraine hills is the most legible in the relief. It begins its course near the Vistula valley, east of Płock. It continues toward the NNW, between Mochowo and Kurowo. Then, at the height of Sierpc, it changes its course to NW-SE. In the southern part, it is less well preserved, reaching up to 11 m in height. On the DEM, it is clearly visible in the northern part, and the hills reach a height of up to 18 m. At some point, this sequence disappears under the fluvio-glacial formations accumulated in the later phase of the ice-sheet extent. On the Urszulewo Plain, between Rembelin and Płock, only fragmentary forms have survived, which may be the remains of moraines.

Numerous arcs of terminal moraines have been preserved in the Dobrzyń Lakeland, described in detail in Teodorski (2023). Generally, in the southern part of the lakeland, the most visible and longest moraine sequence begins in Rembelin and continues to the northwest (Fig. 4). Moraines in this sequence reach up to 15 m in height. North of Dobrzyń, a number of minor end moraines have been interpreted. Moraine hills are most common in the central part of the lakeland. Moraine arcs are characterized by orientation: W-E and WSW-ENE in the southeast, from NE-SW to N-S in the east, and also close to N-S in the west. The moraines in the eastern part of the area are best visible on the model, and they reach a height of up to 17 m. In the northern part of the lakeland, there is a clear sequence of terminal moraines representing the ice limit of three glacial lobes from the Kujawy–Dobrzyń subphase. The lines of these forms are generally oriented on the WSW-ENE line and reach up to 28 m in height.

Grain-size characteristics and petrography of the gravel fraction of glacial tills

The analyzed tills from the sites covered by this research do not show large differences in terms of granulometry. The content of the gravel fraction ranges from 0.29% (Kamień Kotowy, site 27) to 3.63% (Ignackowo, site 20). The content of the sand fraction ranges from 39.53% (Kikoł, site 11) to 57.83% (Sumin, site 9). The exception is the site in Wawrzonkowo (site 8), where the content of this fraction is 15.01%. The total content of the silt and clay fraction ranges from 41.51% to 60.08%, again except at the site in Wawrzonkowo (site 8), where it is 84.67%. In the gravel fraction with a diameter of 5–10 mm, crystalline rocks constitute 33–34% in the southern part of the Dobrzyń Lakeland, 36–44% in the eastern sites in the study area, 48–66% in the northern part of the Dobrzyń Lakeland, and 34–81% in the central part of the Dobrzyń Lakeland. Northern limestones and other carbonate rocks are essentially absent in the northern and central parts of the Dobrzyń Lakeland (except for the sites in Makowiska, site 10; Chlebowo, site 13; and Ignackowo, site 20). In the remaining sites, in most cases, the northern limestone content ranges from 33% to 47%.

AMS

The magnetic susceptibility of tills in the studied sites ranges from 0.97×10^{-4} to 2.73×10^{-4} SI (Table 1). The highest K_m was recorded in the northern part of the Dobrzyń Lakeland ($2.14 \times$

10^{-4} SI), while the lowest K_m was recorded in the Płoński Plateau, last covered by the ice sheet during the Saalian glaciation (1.4×10^{-4} SI). In the studied sites, L rarely exceeds 1% and is in the range of 1,000–1,015. The average L values slightly differ in the northern part of the Dobrzyń Lakeland (1.008) and in the Płoński Plateau (Saalian tills; 1.007). F prevails over L and has a decisive influence on the P_j . The F values for individual stations range from 1,000 to 1,030. The highest average F values were recorded in the southern part of the Dobrzyń Lakeland (1.014) and in the area between the Lakeland and the local LGM extent (1.013). The P_j ranges from 1.003 to 1.038 and reaches the highest values in the regions characterized by the highest F values, assuming the maximum average values of 1.020 (southern part of the Dobrzyń Lakeland). The T parameter has a wide range of values from -0.821 to 0.957 . In the northern part of the Dobrzyń Lakeland and in the area covered by an ice sheet during the Saalian glaciation, L prevails ($T < 0.0$); in the remaining part of the research area, F prevails. The values of S_1 for the mean axis vector k_{\max} range from 0.442 to 0.733. S_1 reaches the highest average values in the northern part of the Dobrzyń Lakeland (0.610), and the lowest values in the southern part of the Dobrzyń Lakeland (0.556). The value of S_1 for the k_{\min} axis ranges from 0.450 to 0.885.

On the basis of the obtained magnetic fabrics, the directions of the ice-sheet movement were determined (Figs. 4 and 5). When lineation is predominant ($T < 0$), the direction of ice-sheet movement is determined parallel to the orientation of the k_{\max} axis. When foliation prevails in the studied location ($T > 0$), k_{\max} axes are dispersed along a (shear) plane, and AMS fabric has a “girdled” pattern. In this situation, the direction of shear (direction of ice-sheet movement) is parallel to the dip direction of the girdle (or imbrication of k_3 axes) similar to the pebble fabric (Benn, 1994; Hooyer et al., 2008; Ives and Iverson, 2019). The girdled pattern of the fabric is characteristic for low shear strain. On the other hand, the AMS fabric is strongly clustered at moderate shear strain (Hooyer et al., 2008). In the second case, two subgroups can be distinguished. In the first subgroup of foliated magnetic fabrics, the orientation of k_{\max} and k_{\min} lies in the direction of ice-sheet movement. The second subgroup concerns fabrics in which the k_{int} and k_{\min} axes lie in the direction of ice-sheet movement.

The orientations of the mean vector of individual magnetic susceptibility axes are presented in Table 1. In the northern part of the Dobrzyń Lakeland, the ice-sheet movement directions range from ENE-WSW in the western part (Steklin, site 7; Wawrzonkowo, site 8) through N-S in the northern part (Mazowsze, site 1; Kijaszkowo, site 2; Klonowo, site 3) to NW-SE in the eastern part (Nowa Wieś, site 4; Wildno, site 5) (Figs. 4 and 5). In the central part of the lakeland, it generally changes from the NNW-SEE in the north (Makowiska, site 10; Janowo, site 12) to more W-E farther in the south (Złotopole, site 14; Karnkowo, site 17; Głodowo, site 19; Ignackowo, site 20; Bałdowo, site 23). In the southern part of the Dobrzyń Lakeland, three mean directions of ice-sheet movement were recorded: WNW-ESE (Nowa Wieś, site 21; Dobrzyń, site 35), WSW-ENE (Wierznica, site 24; Michałkowo, site 26), and SW-NE (Mokowo, site 25; Włocławek, site 34). In the Urszulewo Plain and the area of the Płoński Plateau occupied by the Weichselian glaciation ice sheet, the directions of ice-sheet movement obtained range from NNW-SSE (Rempin, site 29) to SW-NE (Łąkie, site 15). Some order can be observed in the part of the Płoński Plateau occupied by the Saalian glaciation ice sheet. In the northern part, the direction of movement of the

ice sheet is similar to the N-S line (Nowe Piastowo, site 28; Zawidz Kościelny, site 31) and then changes to WNW-ESE or WE (Rychacice, site 30; Kuchary-Jeżewo, site 33).

Rock magnetism

The S -ratio assumes similar values in all sites, from -0.18 to 0.42 (Table 1). In most of the sites, this ratio is slightly positive, which indicates a slight predominance of low-coercivity minerals in the tested samples. The IRM saturation curves take a relatively similar shape (Fig. 6). From the curves, it can be seen that 29–68% of low-coercivity minerals (magnetization in the 0–100 mT field range), 21–36% of medium-coercivity minerals (100–400 mT), and 11–39% of high-coercivity minerals (>400 mT) are responsible for the magnetization of the samples. In many cases, samples do not reach full saturation in a field of 3 T.

In the Lowrie test, the highest magnetization values can be observed on the x-axis (low-coercivity minerals), although the percentage value of this component is variable (Fig. 7). The samples are completely demagnetized at a temperature of 600–700°C. In many samples (e.g., Nowa Wieś, site 4; Moszczonno, site 6; Bałdowo, site 23), a significant decrease in the magnetic remanent on the x-axis and y-axis is noticeable in the temperature range of 100–300°C. The magnetic susceptibility curve shows an increase in value up to a temperature of 200°C, and then a decrease in its value. A relatively uniform decrease in magnetization to the temperature of 550°C is recorded in the samples from the Nowe Piastowo (site 28), Kuchary-Jeżewo (site 33), and Zawidz Kościelny (site 31).

The results of the AARM tests are shown in Figure 8. In the first case (Nowa Wieś, site 4), after using ARM, the AARM axes are more clearly grouped than the AMS axes. The k_{\max} azimuth is generally similar, being 33° for AMS and 32° for AARM. Nevertheless, the inclination of the ellipsoid is different in the two cases. In the case of the AMS, the ellipsoid is inclined toward the NW ($k_{\text{int}} = 293/54$), while the AARM ellipsoid is inclined toward the NE ($k_{\max} = 32/35$). In the second case (Głogi, site 16), after using ARM, the AARM axes are less clearly grouped than the AMS axes. In general, the inclination of the AARM axes ($k_{\max} = 29/10$, $k_{\text{int}} = 294/25$, $k_{\min} = 138/63$) relates by direction and inclination to the orientation of the AMS axis ($k_{\max} = 5/4$, $k_{\text{int}} = 273/31$, $k_{\min} = 102/59$). In the third case (Karnkowo, site 17), again after using ARM, the AARM axes are less clearly grouped than the AMS axes. They are also characterized by a different orientation to the AMS and a differently inclined ellipsoid ($k_{\max} = 216/9$, $k_{\text{int}} = 120/34$, $k_{\min} = 319/55$ for AARM; $k_{\max} = 268/7$, $k_{\text{int}} = 359/8$, $k_{\min} = 138/79$ for AMS). In all three cases, the samples after the use of ARM are characterized by higher values of magnetic susceptibility and a much larger spread on the K_m versus P_j diagram. In Nowa Wieś (site 4) the parameter T has lower values in AARM ($T = -0.192$) than in AMS (0.045); in other cases, it has higher values (0.229 and 0.089 for Głogi, site 16, and 0.372 and 0.144 for Karnkowo, site 17, respectively).

Discussion

Magnetization carriers

Measurements of the IRM show predominantly low-coercivity minerals and some addition of high-coercivity minerals in the tested till samples (Fig. 6, Table 1).

Based on the Lowrie test (Fig. 7), it was found that magnetite and hematite are present in all tested samples. Hematite is also

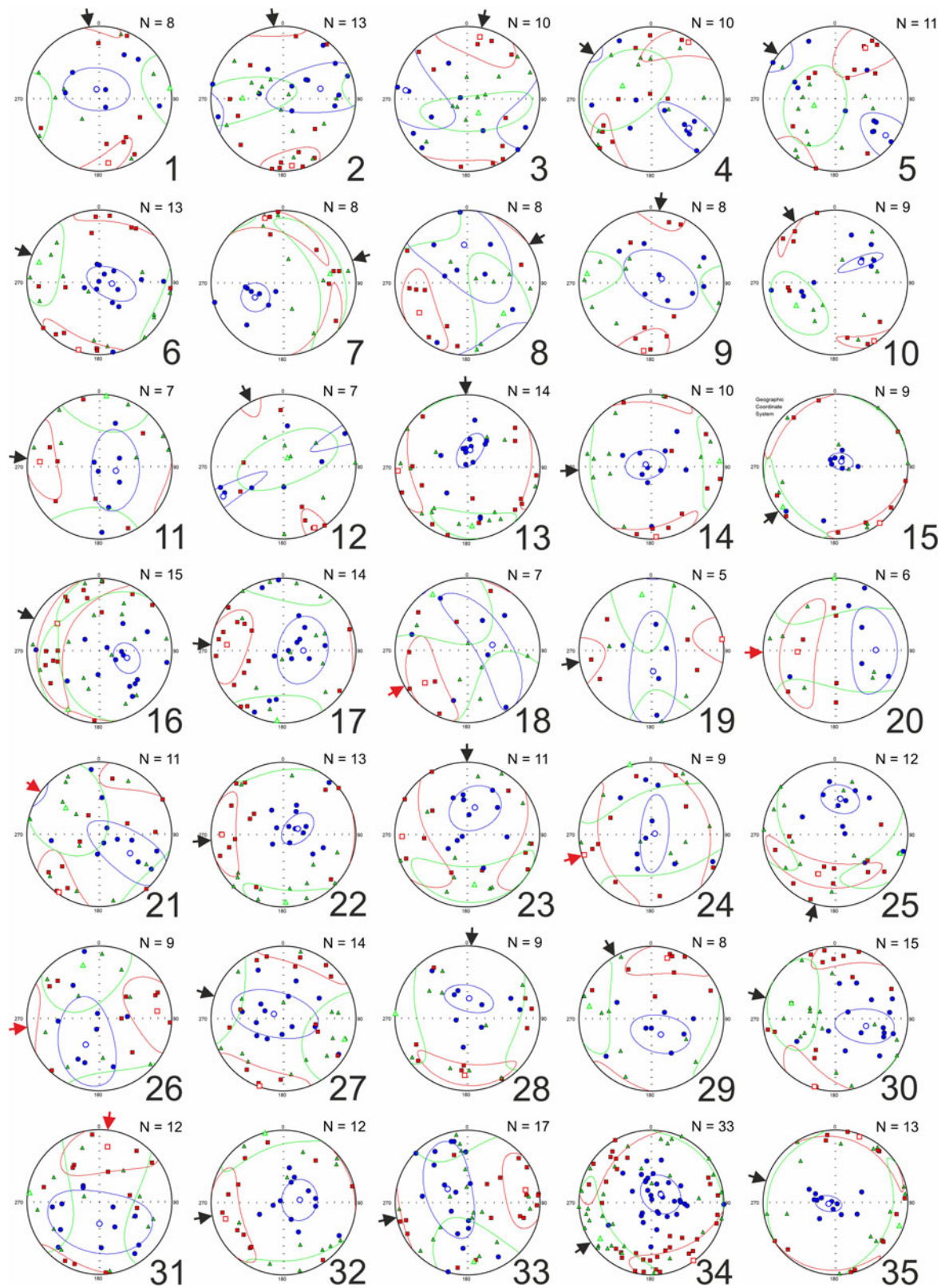


Figure 5. Anisotropy of magnetic susceptibility (AMS) projections in geographic coordinates for individual sites (squares, axis of maximum magnetic susceptibility; triangles, axis of intermediate magnetic susceptibility; circles, axis of minimum magnetic susceptibility) together with the interpreted direction of ice-sheet movement (arrows); red arrows indicate cases where S_1 for the maximum and minimum axes is below 0.6 (weakly oriented axes); see Table 1 for names and numbers of sites.

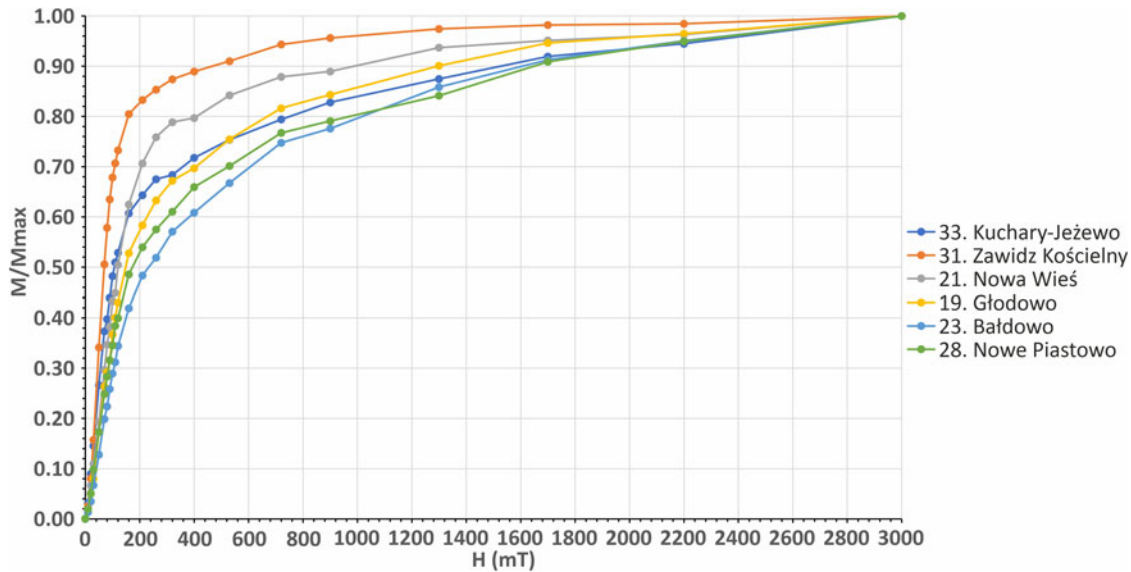


Figure 6. Isothermal remanent magnetization (IRM) saturation curves. M/M_{max} , ratio of magnetization to maximum magnetization; H , value of the applied magnetic field; see Table 1 for names and numbers of sites.

responsible for the fact that samples do not reach full IRM saturation even at a field of 3 T (Fig. 6). Several minerals may be responsible for the significant decrease in magnetization in the x and y curves seen in many samples. The first explanation for this relationship may be related to the presence of iron sulfides in the tested samples. However, the examined tills showing such a relationship (belonging to the Weichselian glaciation) are characterized by a red-brown color, which indicates the oxidation of iron minerals. The second responsible mineral may be titanomagnetite, which is popular in crystalline rocks included in the studied tills. A third mineral may be maghemite, which Hopkins et al. (2016) suggested may account for the marked decrease in magnetization at 200–300°C. Maghemite has been identified in sediments formed in cold environments (Kodama, 1982), including glacial tills (Gentoso et al., 2012). A clear decrease in magnetization on the x-axis and y-axis at 100–300°C recorded in the samples of tills of the Weichselian glaciation is practically absent in the samples of glacial tills of the Saalian glaciation (Nowe Piastowo, site 28; Zawidz Kościelny, site 31; Kuchary-Jeżewo, site 33). This proves that only magnetite and hematite occur in the tills of the older glaciation.

Comparison of AMS and AARM studies (Fig. 8) indicates that, at least in some sites, AMS is not caused by ferromagnetic minerals but by paramagnetic minerals (Jackson, 1991), most likely lamellar, such as minerals from the mica group or clay minerals. The low magnetic susceptibility of the tested till samples ($<5 \times 10^{-4}$ SI) may also indicate that magnetic susceptibility may be mainly controlled by paramagnetic minerals (Hroudá, 2007). The anisotropy of clay minerals comes from their crystallographic structure. Despite this, it has been proven that magnetic lineations are common in clayey rocks. When cracking along the basic plane, these minerals are arranged parallel to the directions of, for example, stretching (Parés and van der Pluijm, 2002; Cifelli et al. 2005, 2009).

The AMS and rock magnetism parameters generally do not correlate directly with the grain-size composition or petrographic composition of the gravel fraction in tills. However, the research indicates that the percentage content of crystalline rocks in the

fine gravel fraction (Kr) may also have an impact on the anisotropy. Changing Kr content shows an inverse correlation with magnetic foliation ($r = -0.58$) and the average degree of anisotropy ($r = -0.58$) (Fig. 9). An increasing percentage content of crystalline rocks is associated with a decrease in carbonate rock content. This may be related to postdepositional weathering processes that may lead to decalcification of the tills in some sites (sites 7, 9, 11, 12, 14, 16–19, 21–23, 27) together with the formation of a certain amount of high-coercivity minerals such as hematite or goethite, which led to a decrease in the degree of anisotropy. However, it seems that high-coercivity minerals did not significantly alter the orientation of principal susceptibility axes.

Condition of till deposition

As noted earlier, there are three types of AMS projections in the studied locations (Fig. 5). In the first case, where L predominates, the k_{max} axis is relatively well ordered, and the other axes of susceptibility are stretched around it (e.g., Kijaszkowo, site 2). In such a situation, the direction of ice-sheet movement was determined based on the orientation of the k_{max} axis. This means that mineral/magnetic grains are arranged with their longest axis parallel to the movement of the ice sheet. The second type of magnetic fabrics concerns the situation in which F prevails in the tested fabrics. In this case, the k_{min} axis is relatively well ordered, and the other axes lie in a plane perpendicular to this axis. The first subtype of foliated AMS is a situation in which the k_{max} and k_{min} axes lie in the direction of the ice-sheet movement (e.g., Karnkowo, site 17; Piątki, site 22). To sum up, in both situations described earlier, the direction of the ice-sheet movement can be determined on the basis of the orientation of the k_{max} axis, despite the fact that the fabrics look different ($T < 0$ or $T > 0$). The mechanism responsible for such arrangement of mineral grains is simple shear (Shumway and Iverson, 2009; Thomason and Iverson, 2009; Fig. 10, I). The direction of shear strain is the result of the horizontal force associated with the movement of the ice sheet and the vertical force associated with the vertical pressure of the ice mass.

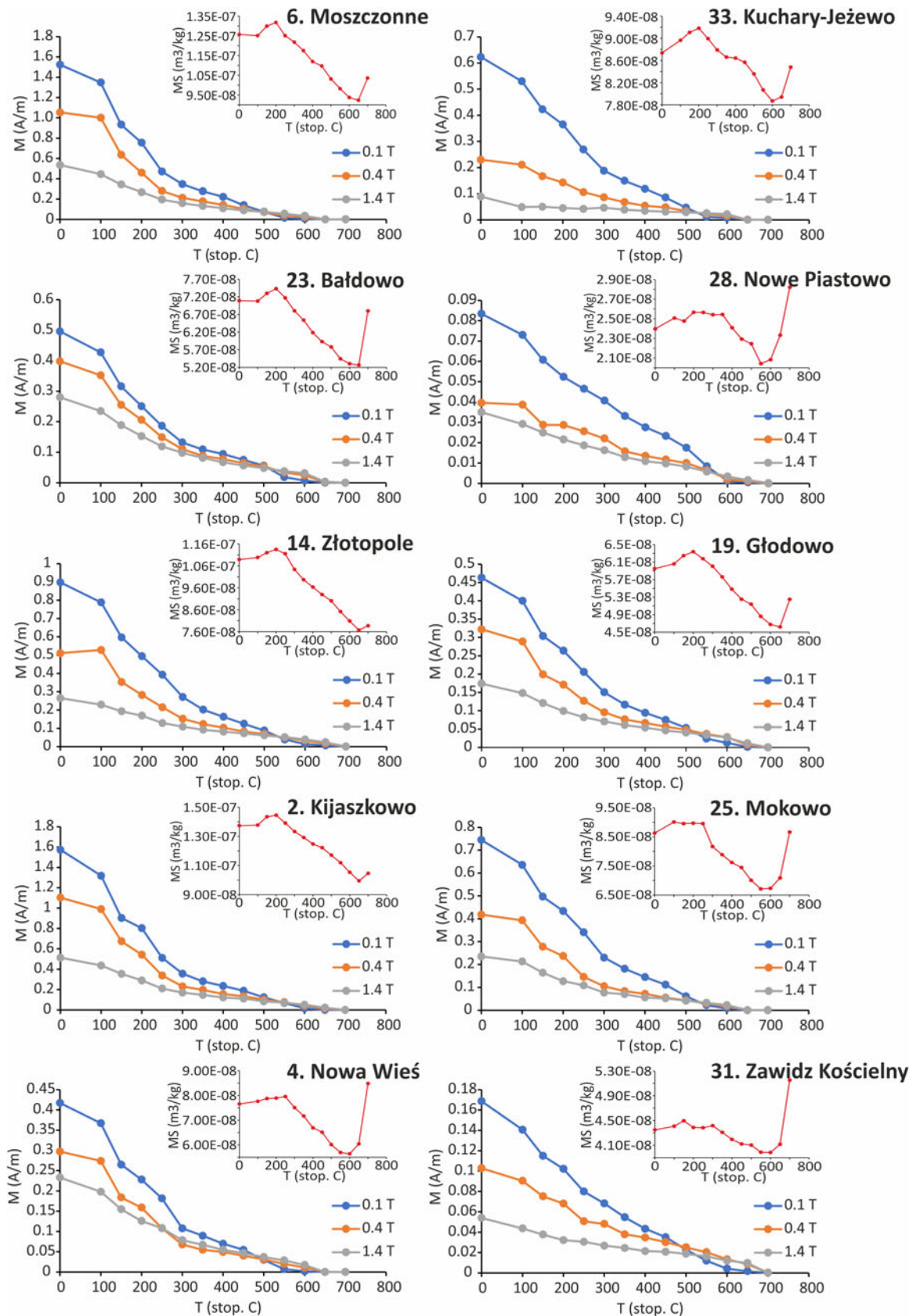
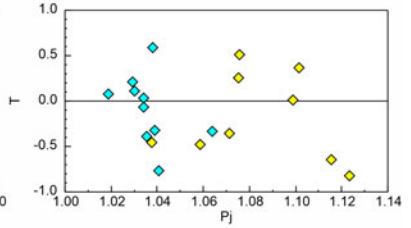
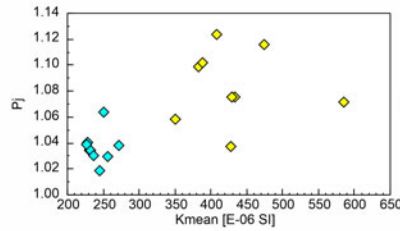
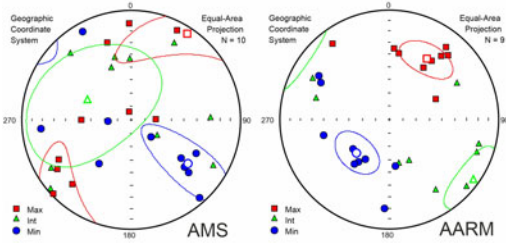
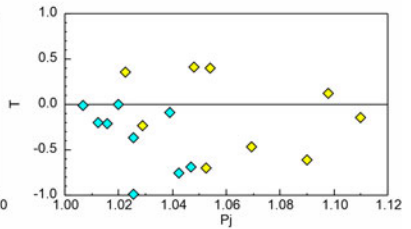
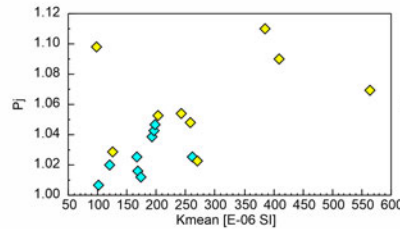
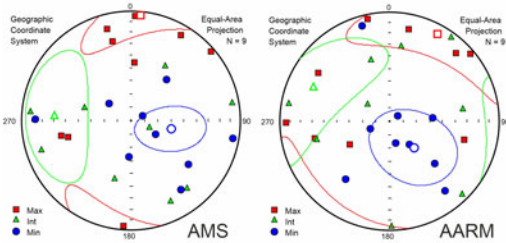


Figure 7. Lowrie test results (blue line, magnetization on the x-axis; orange line, magnetization on the y-axis; gray line, magnetization on the z-axis) along with the change in magnetic susceptibility during individual heating steps of the samples (red line); see Table 1 for names and numbers of sites.

4. Nowa Wieś



16. Głogi



17. Karnkowo

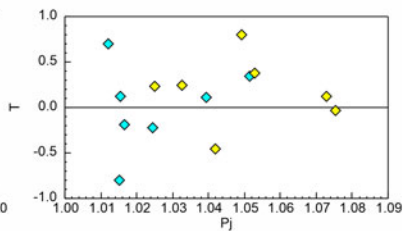
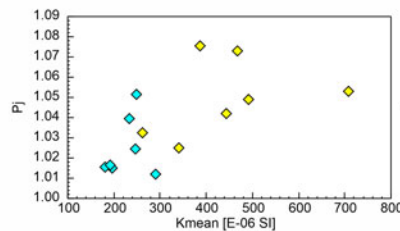
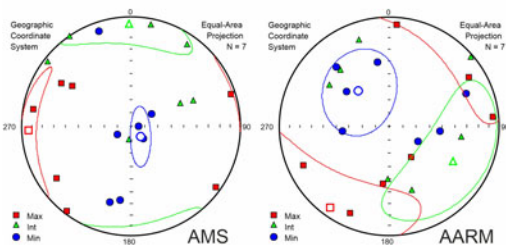


Figure 8. Anisotropy of magnetic susceptibility (AMS) and anhysteretic remanent magnetization (AARM) projections for selected sites (squares, axis of maximum magnetic susceptibility; triangles, axis of intermediate magnetic susceptibility; circles, axis of minimum magnetic susceptibility) with k_m vs. P_j and P_j vs. T graphs (blue points, AMS data; yellow points, AARM data); see Table 1 for names and numbers of sites.

During the laboratory work carried out by Hooyer et al. (2008), no correlation was found between the values of the shear forces acting on the till and the values of the T parameter. This indicates the lack of a direct relationship between the magnitude of simple shear and the type of magnetic fabric. The reason for this may be related to the type of minerals responsible for AMS. Magnetic fabrics with predominant L may be caused by magnetite grains, which are characterized by negative values of the T parameter, while foliation fabrics may be associated with the influence of paramagnetic minerals, including lamellar minerals, on anisotropy (see “Magnetization Carriers”).

Contrary to the value of parameter T , it was shown that the eigenvalues, S_1 , are a good indicator of shear intensity. For fabrics included in the two cases described earlier, the value of S_1 for the k_{\max} axis ranges from 0.442 to 0.733, with an average of 0.585 (Fig. 5, Table 1). Based on research by Hooyer et al. (2008), it can be concluded that the S_1 values obtained indicate a small value of simple shear forces acting during the accumulation of the tested tills. The declining values of simple shear may be a reflection of the weakening dynamics of the ice sheet. The record of slight dynamics of the ice sheet may correlate with the 2 m depth of AMS till sampling. It seems quite possible that the tills of the subsurface layers are a record of a rather final stage of ice-sheet deposition. The degree of orientation of the magnetic

susceptibility axis may also be influenced by the content of the gravel fraction in tills. For example, the highest value of the S_1 eigenvalue for the k_{\max} axis in the range of 0.654–0.733 is found in tills with the smallest gravel fraction content at the level of 0.32–0.65%. One of the lowest values of S_1 eigenvalue for the k_{\max} axis, in the range of 0.422–0.462, refers to tills with the highest gravel fraction content in the range of 2.77–3.63%. It is worth emphasizing, however, that the relationship does not show strong, direct correlations based on the results from all surveyed locations. Of course, it cannot be ruled out that postdepositional processes influenced the arrangement of grains in tills or the formation of new mineral facies, especially in areas with decalcified tills.

In addition to the declination of the k_{\max} axis, which is aligned with the direction of ice-sheet movement, its inclination is also characteristic. Based on laboratory studies (Hooyer et al. 2008), it was found that under the action of simple shear, the k_{\max} axis is inclined at an angle of 16–25° toward the front of the ice sheet, provided the ice sheet was moving on a relatively flat surface, without much variation in the relief. In the studied tills, in individual sites, the average inclination of k_{\max} axis is 4–46° toward the ice-sheet front for some sites and 2–23° in the opposite direction for other sites. This means that only some of the sites (Kikoł, site 11; Karnkowo, site 17; Białowieżyn,

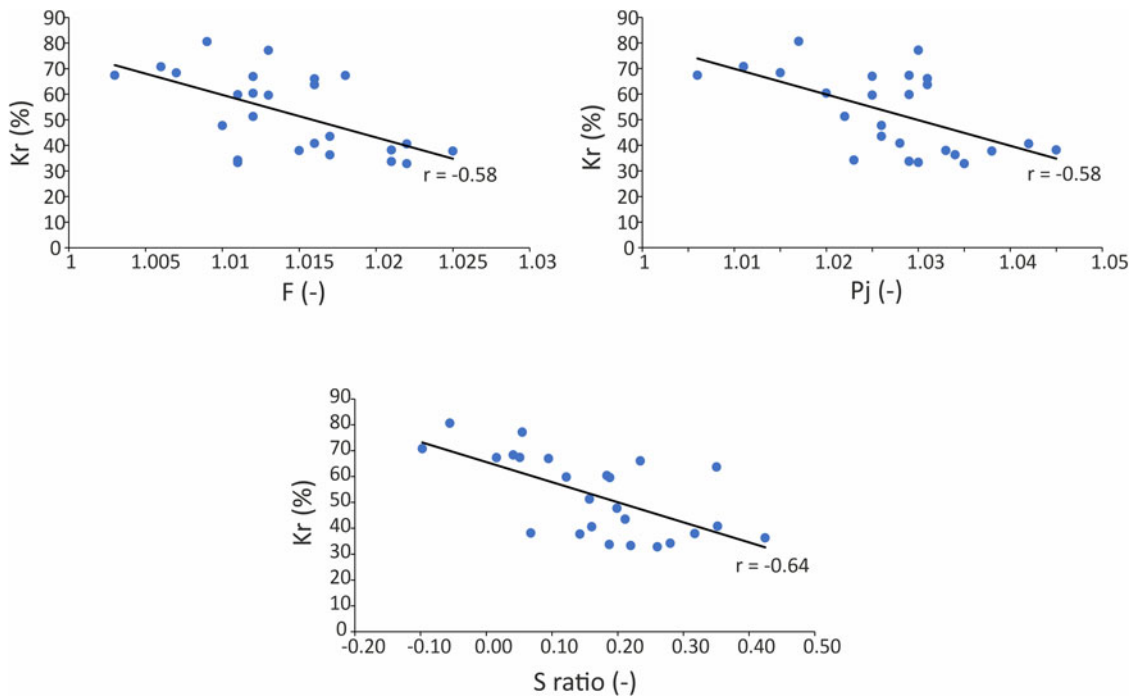


Figure 9. Percentage content of crystalline rocks in gravel fraction (*Kr*) vs. average magnetic foliation (*L*), average degree of anisotropy (*Pj*), and S-ratio for individual sites.

site 18; Piątki, site 22; Zawidz Kościelny, site 31; Stara Biała, site 32) are characterized by a horizontally oriented shear plane, which proves that the ice sheet moved on a relatively flat surface. In the case of the remaining sites, the ice sheet moved along a substrate with a variable inclination (Shumway and Iverson, 2009).

The second subtype of foliated fabrics are those AMS projections in which the k_{int} and k_{min} axes lie in the line of direction of ice-sheet movement (Fig. 5). In this case, the k_{max} axis is oriented perpendicularly or almost perpendicularly to the interpreted direction of ice-sheet movement (e.g., Moszczonze, site 6; Chlebowo, site 13). Such arrangement of the magnetic susceptibility axis may be a record of the action of pure shear on the studied tills (Ankerstjerne et al., 2015; Parés, 2015; McCracken et al., 2016). Pure shear may have acted during the deposition of tills along with simple shear or influenced by glaciectonic deformations on already deposited sediment. As a result of the action of

pure shear, the k_{min} axis aligns with the action of the highest stresses acting on the sediment, while the k_{max} axis aligns with the direction of greatest stretching in the deformed tills (Fig. 10, V).

To sum up, in the studied tills, the arrangement of mineral grains in extreme cases was influenced by: (1) simple shear (Fig. 10, I) combined with subglacial deformations, the basic mechanism associated with the movement of the ice sheet, or (2) pure shear (V) associated with glaciectonic deformations of the deposited sediment. Intermediate states have also been preserved in the tills, that is, a record of two types of shearing (II–IV). Most likely, in this case, the tills were initially deposited by simple shear, and then, as a result of postdepositional glaciectonic processes of varying intensity, the mineral grains were reoriented. It is also worth emphasizing that in the first phases of deformation, only grain reorientation may occur without visible deformation structures.

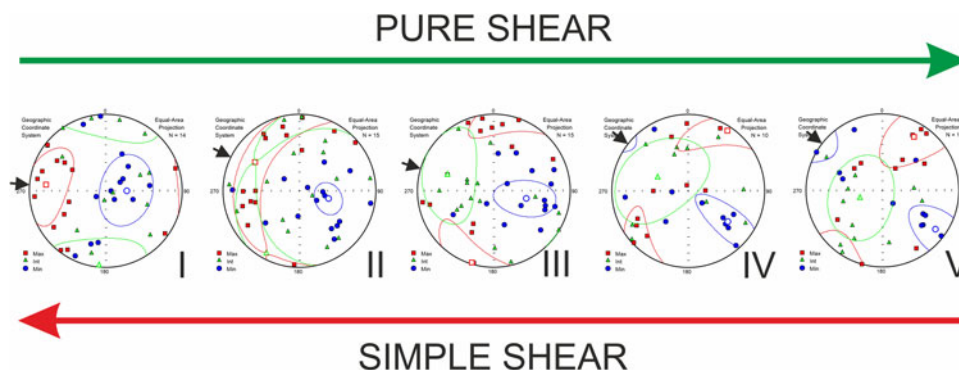


Figure 10. Types of magnetic fabrics (I–V) depending on the distribution of forces acting on the tested tills (squares, axis of maximum magnetic susceptibility; triangles, axis of intermediate magnetic susceptibility; circles, axis of minimum magnetic susceptibility; arrows, interpreted direction of ice-sheet movement).

Directions of ice-sheet movement on the basis of AMS and orientation of glacial landforms on the DEM

The results obtained from the AMS method indicate that in the northern part of the Płoński Plateau, the ice sheet moved from north to south (Nowe Piastowo, site 28; Zawidz Kościelny, site 31), while in the central part of the area, there was a change of direction to WNW-ESE (Rychacice, site 30) or W-E (Kuchary-Jeżewo, site 33) (Figs. 4 and 5). Similar data are also provided by the analysis of the DEM. In the eastern part of the plateau, a network of glacial morpholineaments was identified (Fig. 11). The first of them is located near Drobin. These are extremely elongated depressions of a small depth (up to about 1 m) and strongly elongated hillocks up to about 1 m high (Fig. 11A). In the study area, they stretch for a distance of about 27 km. Their orientation changes from NW-SE in the north to WNW-ESE in the south. Remains of these forms were also located north of Bielsk (orientation WNW-ESE or WE) and northwest of Bielsk (orientation NW-SE). These forms can be classified as megascale glacial lineations (MGLs) (e.g., Newton and Huuse, 2017) on the basis of which it is possible to determine the direction of ice-sheet movement, which in this case is parallel to their course, that is, NW-SE and WNW-ESE. MGLs also appear to occur in moraines located to the northeast of the study area (Fig. 11A, dashed lines), which proves that the ice sheet crossed these moraines. The moraines near Starożreby stand in opposition (Fig. 11A and B, solid lines), which are higher, better preserved, and accumulated on MGLs. This proves that the moraines near Starożreby are younger than those located southeast of Drobin. In the eastern part of the Płoński Plateau,

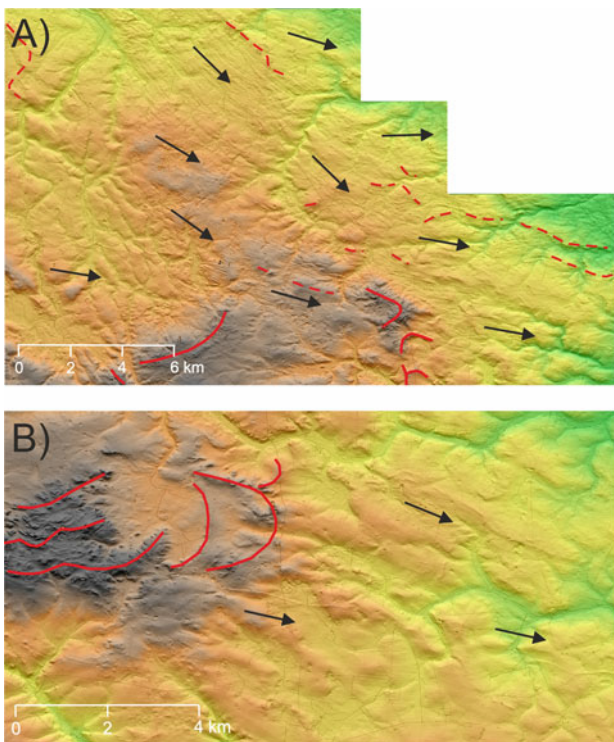


Figure 11. (A) An example of the formation of megascale glacial lineations; (B) relief transformed by the activity of the ice sheet (red lines: solid, sequences of terminal moraines from the Saalian glaciation; dashed, sequences of overridden moraines; arrows, interpreted direction of ice-sheet movement during the Saalian glaciation); location of the outlined area in Fig. 4.

there are also visible elements of the surface shape indicating the transformation of the previously formed relief by the ice sheet (Fig. 11B). These forms are characterized by an elongated, often streamlined shape and orientation along the WNW-ESE or NW-SE line, indicating the direction of ice-sheet movement.

In the Urszulewo Plain and the western part of the Płoński Plateau occupied by the ice sheet during the Weichselian glaciation, the reconstructed directions of ice-sheet movement assume a radial character, typical of the frontal parts of the glacial lobe (Figs. 4 and 5). In the northern part of the described area, north of Tłuchowo, the ice sheet generally moved from SW to NE. This direction is confirmed by the AMS data from the Łąkie (site 15) and the arrangement of glacial meltwater channels and terminal moraines in this region. Between Tłuchowo and Rembelin, the ice sheet moved along a line similar to W-E or WNW-ESE, which is indicated by the arrangement of glacial channel valleys, moraine strings, and AMS data from the Kamień Kotowy (site 27). In the frontal part of the ice sheet, there was a local change in the direction of movement of the ice sheet to NW-SE, which is confirmed by data from the Rempin (site 29; Figs. 4 and 5). In the vicinity of the Vistula valley, between Rembelin and Płock, the ice sheet moved along the NW-SE or WNW-ESE line, parallel to the axis of the Vistula valley. The WSW-ENE direction interpreted in the Stara Biała (site 32) was also recorded in this area. The radial distribution of the ice-sheet movement directions is confirmed by the orientation of the moraine hills in this area (Fig. 4). Also, Skompski (1969) presented similar conclusions based on till clast fabric measurements in available exposures, stating that between Rembelin and Płock the ice sheet moved along the NW-SE line in the immediate vicinity of the Vistula valley, while in the area north of Płock, the direction of ice-sheet movement was from SW to NE or from WSW to ENE.

In the area of the Dobrzyń Lakeland, the directions of ice-sheet movement interpreted on the basis of AMS were compared with the directions obtained on the basis of the analysis of the DEM (Teodorski, 2023). The orientation of the “minor end moraines” and crevasse forms on the DEM indicates that the ice sheet moved from NW to SE between Dobrzyń and Rembelin. AMS data from the Dobrzyń (site 35) confirm this direction of movement of the ice sheet (Figs. 4 and 5). On the other hand, the measurements of clast fabric in till exposures located to the east of Dobrzyń (Skompski, 1969) may indicate local changes in the direction of ice-sheet movement toward more SW-NE or WSW-ESE in the frontal parts of the ice sheet. However, it is currently difficult to reconcile the results of clast fabric measurements with the postulated minor end moraines in the area discussed (Teodorski, 2023), which indicate the direction of ice-sheet movement from NW to SE. In the northern part of this area, in the Michałkowo (site 26), a W-E direction was interpreted. Despite the low strength of the magnetic fabric in this site ($S_1 < 0.6$), this direction is still correct in the context of the arrangement of terminal moraine sequences. At the Mokowo (site 25), the direction of movement on the SSW-NNE line was determined on the basis of the AMS method, that is, almost perpendicular to the one interpreted on the basis of the minor end moraines and crevasse form orientations on the DEM. It is difficult to explain such a direction of movement of the ice sheet. Perhaps the magnetic fabric from this site represents the arrangement of mineral grains in minor end moraines located mainly to the west of this site (Fig. 4, thin red line). The Wierznicza (site 24) is between two strings of minor end moraines. The direction of

ice-sheet movement interpreted on the basis of the AMS method is WSW-ENE and is consistent with the direction of movement determined on the basis of the orientation of minor end moraines. The next AMS site in the southern part of the Dobrzyń Lakeland is located in Włocławek (site 34). The mean direction of ice-sheet movement determined on the basis of the AMS method is SW-NE. On the basis of the crevasse forms and meltwater channel orientation on the DEM model, the perpendicular direction, NW-SE, was interpreted, that is, in line with the mean orientation of k_{\max} axis. Looking at the magnetic fabric in detail from this site, in the orientation of the k_{\max} axis, the component with the N-S orientation is clearly visible. Probably two directions of movement of the ice sheet, NW-SE and S-N, were recorded in the vicinity of the studied site, which resulted in a mean direction of movement from SW to NE. At the Nowa Wieś (site 21), both methods indicate the direction of movement on the NW-SE line.

In the central part of the Dobrzyń Lakeland, the orientation analysis of the terminal moraines, minor end moraines, crevasse forms, eskers, and meltwater channels on the DEM showed a change in the direction of the ice-sheet movement from NW-SE or NNW-SSE in the north to WNW-ESE toward the south. Based on the AMS method, similar conclusions can be drawn (Figs. 4 and 5). The sites located in the north of the region indicate the direction of movement NW-SE (Makowiska, site 10), NNW-SSE (Janowo, site 12), or N-S (Chlebowo, site 13). The sites in the more southern part are characterized by a more latitudinal direction of movement, along the lines WSW-ENE (Białowieżyn, site 18), W-E (Złotopole, site 14; Karnkowo, site 17; Głodowo, site 19; Ignackowo, site 20; Piątki, site 22), and WNW-ESE (Głogi, site 16). Only at the Bałdowo (site 23) is the direction of movement N-S.

In the northern part of the Dobrzyń Lakeland, in the western glacial lobe, based on the orientation of the terminal moraines, minor end moraines, crevasse forms, and meltwater channels on the DEM, it was found that the ice sheet moved from NW-SE in the north to N-S in the south. The AMS data indicate the direction of the ice-sheet movement to N-S (Mazowsze, site 1; Kijaszkowo, site 2). These results correspond with the course of the main glacial channel valley in this area, which proves that the direction of the N-S movement is characteristic of this part of the lobe (Figs. 4 and 5). However, in the northwestern part of the lobe, the NW-SE direction is correct, as evidenced by the orientation of crevasse forms, glacial channel valleys, and moraine hills. In the southern part of the lobe, AMS data indicate radiating directions of ice-sheet movement (Figs. 4 and 5). At the sites of Steklin (site 7) and Wawrzonkowo (site 8), the direction ENE-WSW was recorded; at Sumin (site 9), N-S; and at Moszczonne (site 6) and Kikoł (site 11), WNW-ESE and W-E. Based on the DEM analysis, a series of minor end moraines were determined in this area (Teodorski, 2023), but their general latitudinal orientation indicates the direct direction of the N-S movement. This may indicate that minor end moraines were formed at a different time than the deposition of glacial tills, which is confirmed by studies carried out in the United States (e.g., Cline et al., 2015). On the other hand, the forms interpreted as minor end moraines may actually represent crevasse forms that are parallel to the direction of ice flow interpreted based on AMS samples at sites 7 and 8. In the second central glacial lobe, whose maximum extent is determined by moraines near Chrostkowo, the direction of ice-sheet movement along the NNW-SSE and NW-SE lines in the eastern part of this lobe was interpreted on the basis of the terminal moraines, minor end moraines, and

meltwater channel orientations on the DEM. There are two sites within the described glacial lobe, in Nowa Wieś (site 4) and Wildno (site 5). AMS data from both sites point to the NW-SE direction in the southern part of this lobe. The NNW-SSE ice flow direction is similar to that which can be obtained based on the till fabric measured in the subglacial till building glacial curvilinearities located in the vicinity of Wielgie (Lesemann et al., 2014). The differences between the two methods may result from the fact that in this area, there are no significant areas occupied by glacial plateaus, which makes it difficult to analyze the directions of ice-sheet movement in detail based on the DEM. It seems reasonable to assume that the ice sheet in this glacial lobe, at least in its southern part, moved from NW to SE. New data were also brought by the AMS data from the Klonowo (site 3), which indicate the NNE-SSW direction of movement in the western part of the lobe.

To sum up, the AMS method, in many cases, provides similar information to that obtained from the analysis of the DEM. It also allows the directions of ice-sheet movement to be specified in areas where the glacial relief is not sufficiently developed.

Paleoenvironmental reconstruction of the study area

The study area was eventually covered by an ice sheet during two different glaciations. Most of the Płońsk Plateau was covered for the last time by the ice sheet of the Saalian glaciation. The oldest extent of the ice sheet in the study area is marked by moraines near Bodzanów and northeast of Wyszogród (stage 1; Fig. 12). The latter moraines are well developed and clearly visible on the DEM model. These moraines were formed during one of the recessive phases of the glaciation. The next stage of recession is the stagnation of the ice-sheet front on the line of moraines near Drobin (stage 2; Fig. 12). In the study area, there are hardly any landforms other than moraines, from which it is possible to determine the directions of ice-sheet movement during these two stages. Only on the basis of the orientation of the moraines can it be concluded that the ice sheet moved along a line similar to N-S. The next stage is related to the re-advance of the Saalian glaciation ice sheet. In the northern part of the research area (east of Sierpc), the ice sheet moved from north to south, and then between Drobin and Radzanowo changed its direction to WNW-ESE. The maximum extent of this transgression should be sought east of the study area. During the advance, the ice sheet crossed the moraines near Drobin from the older phase of this glaciation. The occurrence of MGLs on the moraine forms of stage 2 speaks for a later time for this transgression in relation to the previous stages. During the next ice-sheet recession, moraines accumulated near Staroźreby, Radzanowo, and Mochcino (stage 3; Fig. 12). Moraines, in many cases, are well preserved, have a different orientation than those from earlier stages of the ice-sheet existence, and to the northeast of Staroźreby, they lie on MGLs. The next stage is marked by moraines south of Kurowo (stage 4; Fig. 12) and may be a record of a local transgression during the Saalian glaciation or the Weichselian glaciation, as indicated by Dzierżek (2009).

The next stages of the ice-sheet advance are related to the ice sheet of the Weichselian glaciation. In the area close to the local LGM, several sequences of terminal moraine forms were interpreted on the basis of the DEM. The first of them reflects the extent of the ice-sheet front before the local LGM (stage 5a; Fig. 12). Subsequently, transgression occurred, and the ice sheet crossed the previously deposited moraines from stage 5a. The

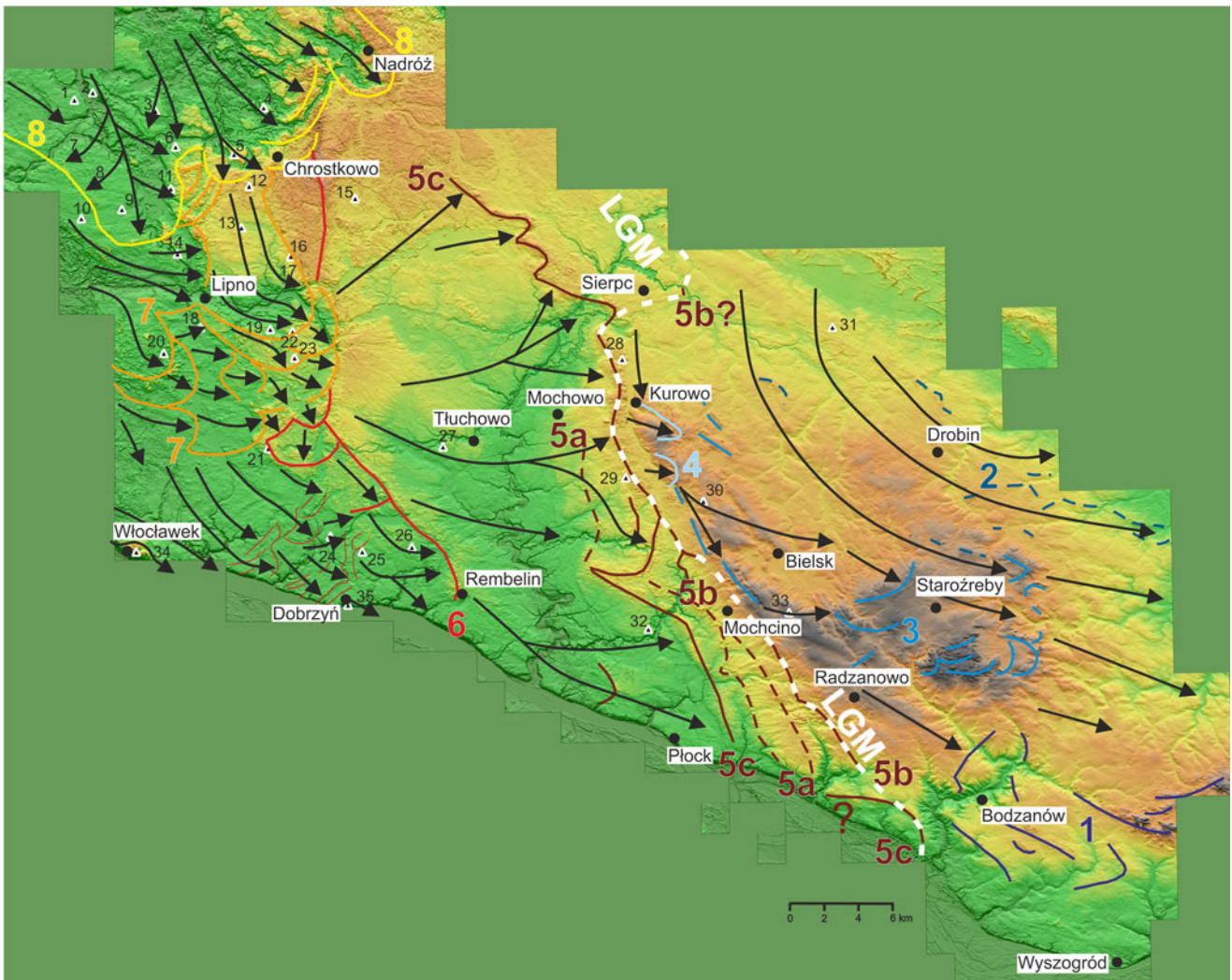


Figure 12. Paleogeographic sketch showing the development and disappearance of the ice sheet of the Saalian and Weichselian glaciations in north-central Poland (colored lines: solid, lines of terminal moraines; dashed lines, lines of overridden moraines; 1–8, stages of the ice-sheet extent; arrows, interpreted direction of ice-sheet movement; LGM, maximum extent of the Weichselian glaciation ice sheet)

existence of overridden moraines in this region is also indicated by Roman (2010). Moraine forms also occur to the northwest and southeast of Mochcino (stage 5b; Fig. 12). They determine the maximum extent of the ice sheet of the Weichselian glaciation in this area. The next stage of the ice-sheet front stillstand can be associated with the best-preserved and longest sequence of terminal moraines (stage 5c; Fig. 12). This sequence is particularly visible in the area north of the Mochowo–Kurowo line. It is debatable whether the sequence of terminal moraines described above can be a record of the local LGM in the northern part of the study area. According to Kotarbiński (1998), in this region, the extent of the ice sheet during the local LGM is determined to the east of Sierpc and is based on the location of the few preserved single terminal moraine hills. This position is also confirmed by Krupiński (2005), who points to two sites of interglacial sediments located north of Sierpc, where sediments belonging to the Eemian interglaciation are covered with glacial till (or its residue) of the Weichselian glaciation. On the other hand, the local LGM line running west of Sierpc is indicated by Lamparski (2001), and it coincides with the location of the described moraine sequence. Undoubtedly, the described series

of moraines in its central part exceeds the local LGM moraines from stage 5b. It is possible that terminal moraines have also been preserved in the southern part of the study area, in the immediate vicinity of the Vistula valley, which would also be a record of this stage of the ice-sheet extent. Possibly occurring moraines may also overprint the moraines from stage 5b. This information suggests that the LGM in north-central Poland is asynchronous. Based on the this, it can be concluded that in the period around the local LGM, there were several oscillations of the ice-sheet front. At that time, the ice sheet was characterized by directions of movement from SW–NE in the north to NW–SE in the south. Due to the accumulation of fluvioglacial sediments on the Urszulewo Plain, there are no terminal moraines that could mark the subsequent stages of ice-sheet recession. In the vicinity of the Vistula valley, between Rembelin and Plock, remains of moraines were interpreted, which Roman (2010) interprets as overridden moraines (Fig. 12).

In the Dobrzyń Lakeland, the period of ice-sheet recession can be divided into three stages, described in detail in Teodorski (2023). In the first stage, the easternmost front of the ice sheet stopped in the vicinity of Rembelin (stage 6; Fig. 12). Dzierżek

(2009) also presents a similar assumption. On the other hand, Roman (2010, 2019) does not describe any terminal moraines in this area, indicating a uniform advance and recession of the ice sheet. Then, the ice sheet gradually retreated from the lakeland. The short-term advance of the ice-sheet front is indicated by minor end moraines between Włocławek (site 34) and Dobrzyń (site 35). The directions of ice-sheet movement generally change from similar to N-S in the north through NW-SE to W-E or locally SSW-NNE in the southeastern part. The next stage (stage 7; Fig. 12) is associated with the transgression of a small ice stream in the central part of the Dobrzyń Lakeland. During this stage, the ice sheet crossed the oldest moraines located in the eastern part of the Dobrzyń Lakeland and the ice sheet generally moved WNW-ESE. The last stage of the ice-sheet extent in the Lakeland (stage 8; Fig. 12) is associated with the transgressive–regressive Kujawy–Dobrzyń subphase (Lamparski 1991; Niewiarowski et al., 1995; Dzierżek, 2009). The ice-sheet front stopped on the line of moraines near Nadróż and Chrostkowo during the last stage of deglaciation. During this subphase, the ice sheet generally moved along the NNW-SSE line. Dzierżek (2009) also determined a similar direction of ice flow based on the orientation of moraine ridges in the northern part of the lakeland. The directions of ice flow obtained in the Dobrzyń Lakeland area generally agree with those obtained by Morawski (2009).

Conclusions

Based on the conducted research, several new conclusions can be drawn about the ice-sheet dynamics in the area of north-central Poland during the Saalian and Weichselian glaciations.

On the basis of the AMS method, it was found that there are magnetic fabrics in the tested tills whose arrangement is due to simple shear, pure shear, or a mixture of the two types. Simple shear is associated with subglacial deformations in the bed of the ice sheet. Pure shear occurs during syn- or postdepositional glaciectonic processes.

The arrangement of mineral grains in the examined tills indicates generally low values of simple shear acting during their deposition, which may be a reflection of the weakening subglacial deformations and the decreasing dynamics of the ice sheet. Glaciectonic processes associated with the action of pure shear indicate a temporary, local increase in ice-sheet activity.

The directions of ice-sheet movement determined on the basis of the AMS method are consistent with the directions of movement interpreted on the basis of the DEM model. This shows that the AMS method can be used for reconstructing regional pattern of the ice flow direction and can yield new data on the Pleistocene glaciations.

The innovative method of sampling glacial tills from under the surface of the plateau turned out to be effective and has a chance to contribute to even greater dissemination of the use of the AMS method in Quaternary studies concerning the determination of ice-sheet movement and reconstructing processes of subglacial till formation.

The composition of the magnetic minerals in tills depends on their age. Magnetite, hematite, titanomagnetite, and/or maghemite have been identified in the tills of the Weichselian glaciation. Tills from the Saalian glaciation contain mainly magnetite and hematite. At least in some cases of the examined tills, paramagnetic minerals, such as some clay minerals or minerals from the mica group, are responsible for AMS.

During the analysis of the DEM, previously unidentified landforms in north-central Poland were determined. Megascale glacial lineations were discovered in the Płoński Plateau. In the area of the local LGM, several sequences of terminal moraine forms, previously not described or only fragmentarily described in this part of Poland, were located.

In the area of the Płoński Plateau, in the generally recessive phase of the Saalian glaciation, the transgression of the ice sheet was interpreted. The ice sheet in the northern part of the Plateau area moved along the N-S line, and then in the central part it changed direction to WNW-ESE. The direction of movement close to latitudinal is perpendicular to the main direction of movement during the recession of the ice sheet of the Saalian glaciation, which indicates a certain distinctiveness of this transgressive glacial stage.

Within the area occupied by the Weichselian ice sheet, four glacial episodes with separate directions of ice-sheet movement can be distinguished: (1) the stage of the maximum extent of the ice sheet; (2) the stillstand of the ice sheet front in the vicinity of Rembelin; (3) the stage of ice-sheet readvance in the central part of the Dobrzyń Lakeland; and (4) the stage of the Kujawy–Dobrzyń subphase.

Acknowledgments. The author is grateful to Michał Bakiera for help with fieldwork. The author would like to thank Sebastian Richiano and an anonymous reviewer for all the comments and suggestions that improved the article. This research did not receive any specific grant from funding agencies in the public, commercial, or not-for-profit sectors.

References

- Ankerstjerne, S., Iverson, N.R., Lagroix, F., 2015. Origin of a washboard moraine of the Des Moines Lobe inferred from sediment properties. *Geomorphology* **248**, 452–463.
- Baraniecka, M.D., 1996. Szczegółowa Mapa Geologiczna Polski w skali 1:50,000, arkusz Raciąż. Państwowy Instytut Geologiczny, Warsaw.
- Benn, D., 1994. Fabric shape and the interpretation of sedimentary fabric data. *Journal of Sedimentary Research* **64**(4a), 910–915.
- Cifelli, F., Mattei, M., Chadima, M., Hirt, A.M., Hansen, A., 2005. The origin of tectonic lineation in extensional basins: combined neutron texture and magnetic analyses on undeformed clays. *Earth and Planetary Science Letters* **235**, 62–78.
- Cifelli, F., Mattei, M., Chadima, M., Lenser, S., Hirt, A.M., 2009. The magnetic fabric in undeformed clays: AMS and neutron texture analyses from the Rif Chain (Morocco). *Tectonophysics* **466**, 79–88.
- Clark, C.D., 1997. Reconstructing the evolutionary dynamics of former ice sheets using multi-temporal evidence, remote sensing and GIS. *Quaternary Science Reviews* **16**, 1067–1092.
- Cline, M.D., Iverson, N.R., Harding, C., 2015. Origin of washboard moraines of the Des Moines Lobe: spatial analyses with LiDAR data. *Geomorphology* **246**, 570–578.
- Dzierżek, J., 2006. Szczegółowa Mapa Geologiczna Polski w skali 1:50,000, arkusz Lipno. Państwowy Instytut Geologiczny, Warsaw.
- Dzierżek, J., 2009. Palaeogeography of selected areas of Poland during the Last Glaciation. *Acta Geographica Lodziensia*, **95**, 1–112.
- Dzierżek, J., Szymanek, M., 2009. Szczegółowa Mapa Geologiczna Polski w skali 1:50,000, arkusz Skepe. Państwowy Instytut Geologiczny, Warsaw.
- Ewertowski, M., Rzeszewski, M., 2006. Using DEM to recognize possible minor stays of Vistulian (Weichselian) ice-sheet margin in the Wielkopolska Lowland. *Quaestiones Geographicae* **25A**, 7–21.
- Fleming, E.J., Stevenson, C.T.E., Petronis, M.S., 2013. New insights into the deformation of a Middle Pleistocene glaciectonised sequence in Norfolk, England through magnetic and structural analysis. *Proceedings of the Geologists' Association* **124**, 834–854.
- Frankiewicz, A., 2009. Szczegółowa Mapa Geologiczna Polski w skali 1:50,000, arkusz Drobin. Państwowy Instytut Geologiczny, Warsaw.

- Frankiewicz, A., 2013. Szczegółowa Mapa Geologiczna Polski w skali 1:50,000, arkusz Mochowo. Państwowy Instytut Geologiczny, Warsaw.
- Fuller, M.D., 1962. A magnetic fabric in till. *Geological Magazine* **99**, 233–237.
- Gentoso, M.J., Evenson, E.B., Kodama, K.P., Iverson, N.R., Alley, R.B., Berti, C., Kozłowski, A., 2012. Exploring till bed kinematics using AMS magnetic fabrics and pebble fabrics: the Weedsport Drumlin Field, New York State, USA. *Boreas* **41**, 31–41.
- Grabowski, J., Bakhmutov, V., Kdýr, Š., Krobicki, M., Pruner, P., Reháková, D., Schnabl, P., Stoykova, K., Wierzbowski, H., 2019. Integrated stratigraphy and palaeoenvironmental interpretation of the Upper Kimmeridgian to Lower Berriasian pelagic sequences of the Velykyi Kamianets (Pieniny Klippen Belt, Ukraine). *Palaeogeography, Palaeoclimatology, Palaeoecology* **532**, 109216.
- Hodge, V.J., Austin, J., 2004. A survey of outlier detection methodologies. *Artificial Intelligence Review* **22**, 85–126.
- Hooyer, T.S., Iverson, N.R., Lagroix, F., Thomason, F., 2008. Magnetic fabric of sheared till: a strain indicator for evaluating the bed deformation model of glacier flow. *Journal of Geophysical Research* **113**, F02002.
- Hopkins, N.R., Kleman, J., Evenson, E.B., Kodama, K.P., 2016. An anisotropy of magnetic susceptibility (AMS) fabric record of till kinematics within a Late Weichselian low Baltic till, southern Sweden. *Boreas* **45**, 846–860.
- Hrouda, F., 1982. Magnetic anisotropy of rocks and its application in geology and geophysics. *Geophysical Surveys* **5**, 37–82.
- Hrouda, F., 2007. Magnetic susceptibility, anisotropy. In: Gubbins, D., Herrero-Bervera, E. (Eds.), *Encyclopedia of Geomagnetism and Paleomagnetism*. Springer, Dordrecht, Netherlands, pp. 546–560.
- Ives, L.R.W., Iverson, N.R., 2019. Genesis of glacial flutes inferred from observations at Múlajökull, Iceland. *Geology* **47**, 387–390.
- Jackson, M., 1991. Anisotropy of magnetic remanence: a brief review of mineralogical sources, physical origins, and geological applications, and comparison with susceptibility anisotropy. *Pure and Applied Geophysics* **136**, 1–28.
- Jelínek, V., 1978. Statistical processing of anisotropy of magnetic susceptibility measured on groups of specimens. *Studia Geophysica et Geodaetica* **22**(1), 50–62.
- Jorgensen, F., Piotrowski, J.A., 2003. Signature of the Baltic Ice Stream on Funen Island, Denmark during the Weichselian glaciation. *Boreas* **32**, 242–255.
- Kacprzak, L., Lisicki, S., 2005. Szczegółowa Mapa Geologiczna Polski w skali 1:50,000, arkusz Bulkowo. Państwowy Instytut Geologiczny, Warsaw.
- Kacprzak, L., Lisicki, S., 2011. Objasnienia do Szczegółowej Mapy Geologicznej Polski w skali 1:50,000, arkusz Bulkowo. Państwowy Instytut Geologiczny, Warsaw.
- King, E.C., Pritchard, H.D., Smith, A.M., 2016. Subglacial landforms beneath Rutford Ice Stream, Antarctica: detailed bed topography from ice-penetrating radar. *Earth System Science Data* **8**, 151–158.
- Kodama, K.P., 1982. Magnetic effects of maghemitization of Plio-Pleistocene marine sediments, northern California. *Journal of Geophysical Research* **87**, 7113–7125.
- Kotarbiński, J., 1998. Szczegółowa Mapa Geologiczna Polski w skali 1:50,000, arkusz Sierpc. Państwowy Instytut Geologiczny, Warsaw.
- Kozarski, S., 1995. Deglaciation of northwestern Poland: environmental conditions and geosystem transformation (~ 20 ka–10 ka BP). *Dokumentacja Geograficzna* **1**, 1–82.
- Król, E., Wachecka-Kotkowska, L., 2015. Anisotropy of magnetic susceptibility as a potential tool of palaeocurrent direction of the glacial sediments in the Piotrków Trybunalski, Radomsko and Przedbórz area (Central Poland). *Acta Geographica Lodziana* **103**, 79–98.
- Krupiński, K.M., 2005. The investigations of the Younger Pleistocene lacustrine sediments of the Plock Upland. *Prace Państwowego Instytutu Geologicznego* **148**, 1–58.
- Kucharska, M., Wasiluk, R., 2005. Szczegółowa Mapa Geologiczna Polski w skali 1:50,000, arkusz Wyszogród. Państwowy Instytut Geologiczny, Warsaw.
- Lamparski, Z., 1978. Szczegółowa Mapa Geologiczna Polski w skali 1:50,000, arkusz Mochowo. Państwowy Instytut Geologiczny, Warsaw.
- Lamparski, Z., 1980. Szczegółowa Mapa Geologiczna Polski w skali 1:50,000, arkusz Tłuchowo. Państwowy Instytut Geologiczny, Warsaw.
- Lamparski, Z., 1985. Szczegółowa Mapa Geologiczna Polski w skali 1:50,000, arkusz Fabianki. Państwowy Instytut Geologiczny, Warsaw.
- Lamparski, Z., 1991. Loby lodowcowe w kopalnej i obecnej rzeźbie Pojezierza Dobrzyńskiego. In: Kostrzewski, A. (Ed.), *Geneza, litologia i stratygrafia osadów czwartorzędowych*. Wydawnictwa UAM, seria Geografia, Poznań, pp. 105–115.
- Lamparski, Z., 2001. Zarys budowy geologicznej i charakterystyka rzeźby Wysoczyzny Płockiej i Pojezierza Dobrzyńskiego ze szczególnym uwzględnieniem budowy i genezy drumlinów oraz moren czołowych. In: Dzierżek, J. (Ed.), *Rzeźba i osady czwartorzędu środkowo-wschodniej Polski*. Przewodnik do ćwiczeń z geomorfologii i geologii czwartorzędu. Uniwersytet Warszawski, Wydział Geologii, Warsaw, pp. 54–58.
- Leseman, J.E., Piotrowski, J.A., Wysota, W., 2014. Genesis of the “glacial curvilinear” landscape by meltwater processes under the former Scandinavian Ice Sheet, Poland. *Sedimentary Geology* **312**, 1–18.
- Lisicki, S., 2003. Lithotypes and lithostratigraphy of tills of the Pleistocene in the Vistula drainage basin area Poland. *Prace Państwowego Instytutu Geologicznego* **177**, 1–105.
- Lowrie, W., 1990. Identification of ferromagnetic minerals in a rock by coercivity and unblocking temperature properties. *Geophysical Research Letters* **17**, 159–162.
- Lyczewska, J., 1973. Szczegółowa Mapa Geologiczna Polski w skali 1:50,000, arkusz Ciechocinek. Państwowy Instytut Geologiczny, Warsaw.
- Marks, L., 1988. Relation of substrate to the Quaternary palaeorelief and sediments, western Mazury and Warmia. *Kwartalnik AGH, Geologia* **14**, 76s.
- Marks, L., 2012. Timing of the Late Vistulian (Weichselian) glacial phases in Poland. *Quaternary Science Reviews* **44**, 81–88.
- Marks, L. (Ed.), 2022. *Mapa geologiczna Polski w skali 1:500 000. Mapa powierzchni terenu*. Państwowy Instytut Geologiczny, Warsaw.
- Marks, L., Bitinas, A., Błaszkiwicz, M., Börner, A., Guboyte, R., Rinterknecht, V., Tylmann, K., 2022. Northern central Europe: glacial landforms from the Last Glacial Maximum. In: Palacios, D., Hughes, P.D., García-Ruiz, J.M., Andrés, N. (Eds.), *European Glacial Landscapes. Maximum Extent of Glaciation*. Elsevier, Amsterdam, pp. 381–388.
- Marks, L., Dzierżek, J., Janiszewski, R., Kaczorowski, J., Lindner, L., Majecka, A., Makos, M., Szymanek, M., Tołoczko-Pasek, A., Woronko, B., 2016. Quaternary stratigraphy and palaeogeography of Poland. *Acta Geologica Polonica* **66**, 403–427.
- Marks, L., Karabanov, A., Nitychoruk, J., Bahdasarau, M., Krzywicki, T., Majecka, A., Pochocka-Szwarc, K., et al., 2018. Revised limit of the Saalian ice sheet in central Europe. *Quaternary International* **478**, 59–74.
- McCracken, R.G., Iverson, N.R., Benediktsson, Í.Ö., Schomacker, A., Zoet, L.K., Johnson, M. D., Hooyer, T.S., Ingólfsson, Ó., 2016. Origin of the active drumlin field at Múlajökull, Iceland: new insights from till shear and consolidation patterns. *Quaternary Science Reviews* **148**, 243–260.
- Mojski, E., 1958. Szczegółowa Mapa Geologiczna Polski w skali 1:50,000, arkusz Włocławek. Państwowy Instytut Geologiczny, Warsaw.
- Mojski, J.E., 2005. *Ziemia Polskie w czwartorzędzie—zarys morfogenezy*. Państwowy Instytut Geologiczny, Warsaw.
- Morawski, W., 2009. Reconstruction of the Vistula ice stream during the Last Glacial Maximum in Poland. *Geological Quarterly* **53**, 305–316.
- Mycielska-Dowgiałło, E., Rutkowski, J., 1995. *Researches of Quaternary Sediments. Some Methods and Interpretation of the Results*. Wydział Geografii i Studiów Regionalnych Uniwersytetu Warszawskiego, Państwowy Instytut Geologiczny—Państwowy Instytut Badawczy, Komitet Badań Czwartorzędu Polskiej Akademii Nauk, Warsaw.
- Narloch, W., Werner, W., Tylmann, K., 2021. Deformation mechanisms and kinematics of a soft sedimentary bed beneath the Scandinavian Ice Sheet, north-central Poland, revealed by magnetic fabrics. *Sedimentary Geology* **416**, 105862.
- Nechay, W., 1927. Utwory lodowcowe Ziemi Dobrzyńskiej. *Sprawozdania Państwowego Instytutu Geologicznego* **4**, 1–76.
- Newton, A.M.W., Huuse, M., 2017. Glacial geomorphology of the central Barents Sea: implications for the dynamic deglaciation of the Barents Sea Ice Sheet. *Marine Geology* **387**, 114–131.

- Niewiarowski, W., Olszewski, A., Wysota, W., 1995. The role of subglacial features in glacial morphogenesis of Kujawy-Dobrzyń subphase area in the southern and eastern part of the Chełmno-Dobrzyń Lakeland. *Quaternary Studies in Poland* **13**, 65–76.
- Opdyke, N.D., Channell, J.E.T., 1996. *Magnetic Stratigraphy*. Academic Press, San Diego.
- Parés, J.M., 2015. Sixty years of anisotropy of magnetic susceptibility in deformed sedimentary rock. *Frontiers in Earth Science* **3**, 1–12.
- Parés, J.M., van der Pluijm, B.A., 2002. Evaluating magnetic lineations (AMS) in deformed rocks. *Tectonophysics* **350**, 283–298.
- Raunholm, S., Sejrup, H.P., Larsen, E., 2003. Lateglacial landform associations at Jaren (SW Norway) and their glaci-dynamic implications. *Boreas* **32**, 462–475.
- Roman, M., 2010. Reconstruction of the Płock ice-lobe during the Last Glaciation. *Acta Geographica Lodziensia* **96**, 1–171.
- Roman, M., 2019. Ice-flow directions of the last Scandinavian Ice Sheet in central Poland. *Quaternary International* **501**, 4–20.
- Różański, P., Włodek, M., 2009. Szczegółowa Mapa Geologiczna Polski w skali 1:50,000, arkusz Staroźreby. Państwowy Instytut Geologiczny, Warsaw.
- Różański, P., Włodek, M., 2012. Objaśnienia do Szczegółowej Mapy Geologicznej Polski w skali 1:50,000, arkusz Staroźreby. Państwowy Instytut Geologiczny, Warsaw.
- Rühle, E., 1957. Mapa utworów czwartorzędowych Polski w skali 1:2 000 000. *Biuletyn Instytutu Geologicznego* **118**, 489–550.
- Rychel, J., Morawski, M., 2017. Postglacial morpholineaments as an indicator of ice sheet dynamics during the Saale Glaciation in the Białystok Plateau and Sokółka Hills (NE Poland). *Geological Quarterly* **61**, 334–349.
- Shumway, J.R., Iverson, N.R., 2009. Magnetic fabrics of the Douglas Till of the Superior lobe: exploring bed-deformation kinematics. *Quaternary Science Reviews* **28**, 107–119.
- Skompski, S., 1968. Szczegółowa Mapa Geologiczna Polski w skali 1:50,000, arkusz Dobrzyń. Państwowy Instytut Geologiczny, Warsaw.
- Skompski, S., 1969. Stratygrafia osadów czwartorzędowych wschodniej części Kotliny Płockiej. *Biuletyn Instytutu Geologicznego* **220**, 175–258.
- Skompski, S., Słowiński, W., 1962. Szczegółowa Mapa Geologiczna Polski w skali 1:50,000, arkusz Płock. Państwowy Instytut Geologiczny, Warsaw.
- Solon, J., Borzyszkowski, J., Bidlasik, M., Richling, A., Badora, K., Balon, J., Brzezińska-Wójcik, T., et al., 2018. Physico-geographical mesoregions of Poland: verification and adjustment of boundaries on the basis of contemporary spatial data. *Geographia Polonica* **91**, 143–170.
- Stachowska, A., Łoziński, M., Śmigielski, M., Wysocka, A., Jankowski, L., Ziółkowski, P., 2020. Anisotropy of magnetic susceptibility as an indicator for palaeocurrent analysis in folded turbidites (Outer Western Carpathians, Poland). *Sedimentology* **67**, 3783–3808.
- Stewart, R.A., Bryant, D., Sweat, M.J., 1988. Nature and origin of corrugated ground moraine of the Des Moines Lobe, Story County, Iowa. *Geomorphology* **1**, 111–130.
- Stober, J.C., Thompson, R., 1979. An investigation into the source of magnetic minerals in some Finnish lake sediments. *Earth and Planetary Science Letters* **45**, 464–474.
- Stokes, C.R., Tarasov, L., Blomdin, R., Cronin, T.M., Fisher, T.G., Gyllencrutz, R., Hättestrand, C., et al., 2015. On the reconstruction of palaeo-ice sheets: recent advances and future challenges. *Quaternary Science Reviews* **125**, 15–49.
- Stupavsky, M., Gravenor, C.P., 1975. Magnetic fabric around boulders in till. *Geological Society of America Bulletin* **86**, 1534–1536.
- Teodorski, A., 2023. Palaeogeographic reconstruction of the Late Weichselian ice sheet in north-central Poland based on relief analysis. *Journal of Quaternary Science* **38**, 647–657.
- Teodorski, A., Dzierżek, J., Ziółkowski, P., 2021. Reconstruction of subglacial depositional conditions based on the anisotropy of magnetic susceptibility: an example from Dęba (central Poland). *Journal of Quaternary Science* **36**, 391–402.
- Thomason, J.F., Iverson, N.R., 2009. Deformation of the Batestown till of the Lake Michigan lobe, Laurentide ice sheet. *Journal of Glaciology* **55**, 131–146.
- Tylmann, K., Rinterknecht, V.R., Woźniak, P.P., Bourlès, D., Schimmelpfennig, I., Guillou, V., ASTER Team, 2019. The Local Last Glacial Maximum of the southern Scandinavian Ice Sheet front: cosmogenic nuclide dating of erratics in northern Poland. *Quaternary Science Reviews* **219**, 36–46.
- Tylmann, K., Wysota, W., Piotrowski, J.A., 2013. Zastosowanie pomiarów anizotropii podatności magnetycznej (AMS) w badaniach glin subglacialnych. In: XX Konferencja Stratygrafia Plejstocenu Polski. Lasocin, Poland.
- Woodcock, N.H., 1977. Specification of fabric shapes using an eigenvalue method. *GSA Bulletin* **88**, 1231–1236.
- Wysota, W., 2006. Szczegółowa Mapa Geologiczna Polski w skali 1:50,000, arkusz Golub-Dobrzyń. Państwowy Instytut Geologiczny, Warsaw.
- Wysota, W., Lankauf, K.R., Szymańska, J., Chruścińska, A., Oczkowski, H.L., Przegiętka, K.R., 2002. Chronology of the Vistulian (Weichselian) glacial events in the Lower Vistula region, middle-north Poland. *Geochronometria* **21**, 137–142.
- Wysota, W., Sokołowski, R., 2009. Szczegółowa Mapa Geologiczna Polski w skali 1:50,000, arkusz Rypin. Państwowy Instytut Geologiczny, Warsaw.